Characteristics of quasifission products within the dinuclear system model

G. G. Adamian,[1,2,3] N. V. Antonenko,[1,2] and W. Scheid[1]
[1]*Institut für Theoretische Physik der Justus-Liebig-Universität, D-35392 Giessen, Germany*
[2]*Joint Institute for Nuclear Research, 141980 Dubna, Russia*
[3]*Institute of Nuclear Physics, 702132 Tashkent, Uzbekistan*
(Received 25 February 2003; published 2 September 2003)

A new procedure is developed for calculating the charge, mass, and kinetic energy distributions of quasifission products. The quasifission is treated within a transport model which describes a master equation for the evolution of the dinuclear system in charge and mass asymmetries and its decay along the internuclear distance. The calculated yields of quasifission products and their distributions in kinetic energy are in agreement with recent experimental data of hot fusion reactions leading to superheavy nuclei. The importance of shell and deformation effects in quasifission is noted. The preneutron and postneutron emissions as well as the fission of a heavy nucleus in the dinuclear system are considered.

DOI: 10.1103/PhysRevC.68.034601 PACS number(s): 25.70.Jj, 24.10.−i, 24.60.−k

I. INTRODUCTION

Recent experiments on quasifission in fusion reactions leading to superheavy nuclei [1] extended the number of reactions investigated previously [2–6]. In the quasifission process, one finds large mass rearrangements between the interacting heavy ions occurring in a short time [1–6]. The experimental signatures of this process are large widths of mass distributions and an enhanced angular anisotropy, incompatible with compound nucleus fission. Quasifission means the fission of a dinuclear configuration without forming the compound nucleus. It conceptually bridges the gap [7] between deep-inelastic collisions, where the reaction partners come into close contact and exchange many particles without altering their average mass and charge [8–11], and the complete fusion process where the reaction partners lose their identity after forming the compound nucleus. The most important result of the new experiments [1] is the clear evidence of the influence of shell effects in the mass, charge, and kinetic energy distributions of quasifission products.

As shown in Refs. [12–18], quasifission and fusion processes can be described as an evolution of a dinuclear system (DNS), which is formed in the entrance channel during the capture stage of the reaction after dissipation of the kinetic energy of the collision. We assume that the decay of the DNS, which evolves in the mass and charge asymmetry coordinates, gives an adequate description of the charge, mass, and kinetic energy distributions of the quasifission products. The basic assumptions of the DNS model have been microscopically proved in Refs. [19]. The DNS model calculations [13] of evaporation residue cross sections for the cold and hot fusion reactions leading to heavy and superheavy nuclei are in a good agreement with the experimental data [20–22]. Our first estimate of cross section for the $^{48}Ca+^{244}Pu \rightarrow ^{292}114$ reaction was performed before the experiments were conducted and was in perfect agreement with the latter data [21]. The latest experimental data on the production of the nucleus with $Z=118$ in the $^{86}Kr+^{208}Pb$ reaction are consistent with our early predictions.

The quasifission process in heavy nuclear systems gives detailed information about the dynamics of the DNS. In the DNS model, which is used to calculate fusion cross sections for heavy and superheavy nuclei, one assumes that the nuclei exchange nucleons or clusters in a touching position without amalgamating to a compound nucleus. The basic condition for this process is the conservation of individuality of the nuclei [19]. The main ingredients of the DNS model are the inner fusion barrier in mass asymmetry coordinate, which hinders the fusion and the quasifission barrier in the relative distance. Due to the quasifission barrier, the DNS lives for enough time for the development of the diffusion process in the mass asymmetry coordinate. Quasifission distributions reveal sensitive signatures of the dynamical behavior of the DNS and, therefore, are important for a deeper foundation of the DNS model, in addition to the agreement of calculated evaporation cross sections for superheavy nuclei with experimental data.

The quasifission process was already treated with the DNS model in a microscopical transport approach [16,17]. This approach allowed us to describe the charge and mass distributions of the quasifission products for the first time by considering the mass asymmetry degree of freedom only. In the present paper, we essentially extend the transport model by taking more degrees of freedom in the DNS into account, namely, the neutron and proton asymmetry degrees of freedom jointly, and the deformation and angular momentum degrees of freedom effectively. The characteristics of mass, charge and kinetic energy distributions of quasifission products will be calculated and compared with available experiment data.

In spite of an intensive experimental study of the quasifission process, no microscopical model besides the one in Refs. [15–17] was elaborated to our knowledge for calculating the characteristics of quasifission products. In Sec. II of this paper, we extend our model [16,17] to more degrees of freedom. The results of the calculations in comparison with experimental data are shown in Sec. III. A summary is given in Sec. IV.

II. MODEL

A. Evolution of the DNS in charge and mass asymmetry coordinates

The DNS model [12–14] assumes that the compound nucleus is reached by a series of transfers of nucleons or

small clusters from the light nucleus to the heavier one in a touching configuration of the nuclei. The dynamics of fusion is considered as a diffusion of the DNS in the charge and mass asymmetry coordinates, which are here fixed by the charge and mass numbers Z and A_P of the light fragment of the DNS. The inner barrier B^*_{fus} of the potential in the coordinates Z or A_P supplies a hindrance for the fusion in the DNS model.

The DNS model suggested in Refs. [13,14] allowed us to describe the fusion probability P_{CN} and the total quasifission cross section σ_{qf}, and to calculate the charge and mass distributions of the quasifission products [16,17]. Here, we suggest a new variant of the DNS model for the quasifission process which describes both degrees of freedom, the charge and mass degrees of freedom, i.e., explicitly. This is a step forward with respect to the former DNS model which connected the mass and charge asymmetry coordinates and treated the mass or charge coordinate only. In the new model, the DNS simultaneously evolves in Z and A_P by a transfer of protons and neutrons between the nuclei and in R by decay into the direction of an increasing internuclear distance.

In order to derive master equations for the dynamics of the mass and charge transfer, we start with the single-particle Hamiltonian of the DNS:

$$H(\mathbf{R})=\sum_{i=1}^{A_{tot}}\left(-\frac{\hbar^2}{2m}\Delta_i+U_P(\mathbf{r}_i-\mathbf{R})+U_T(\mathbf{r}_i)\right), \qquad (1)$$

where m is the nucleon mass and $A_{tot}=A_P+A_T$ the total mass number of the DNS. The mean single-particle potentials U_P and U_T of the light and heavy nucleus, respectively, include both nuclear and Coulomb fields. Then, we can approximately write in the second-quantization representation of Eq. (1)

$$H=H_{in}+V_{int}, \qquad (2)$$

where

$$H_{in}=\sum_P \epsilon_P a_P^\dagger a_P+\sum_T \epsilon_T a_T^\dagger a_T \qquad (3)$$

and

$$V_{int}=\sum_{P,T}\left[g_{PT}(R)a_P^\dagger a_T+\text{H.c.}\right] \qquad (4)$$

describe the internal states of the DNS nuclei and the transitions of nucleons between the DNS nuclei due to the action of the mean field, respectively. Here, the indices P and T are quantum numbers characterizing the proton and neutron single-particle states with energies ϵ_P and ϵ_T in the light and heavy nuclei, respectively. The R dependence of the transition matrix elements $g_{PT}(R)=\frac{1}{2}\langle P|U_P+U_T|T\rangle$ is replaced by $R=R_m$ in the following where $R_m(Z,N)$ is the R distance of the dinuclear potential minimum and is defined below. Since for the reaction times considered here the thermal equilibrium is established in the DNS, we ignore in Eq. (2) the terms $\Sigma_{P\neq P'}\langle P|U_T|P'\rangle a_P^\dagger a_{P'}$ and $\Sigma_{T\neq T'}\langle T|U_P|T'\rangle a_T^\dagger a_{T'}$ corresponding to the particle-hole transitions between levels in one nucleus under the influence of the mean field of the partner nucleus.

The DNS is characterized by its total energy $E_n^{Z,N}$, the charge and neutron numbers Z and N of the light fragment and the corresponding numbers of the heavy fragments. The additional quantum number n distinguishes the states of the DNS with the same energy, charge, and mass asymmetries. We denote $P_{Z,N}(n,t)$ as the probability of finding the DNS at time t in state (Z,N,n). In the transport approach, this probability can be found by means of the equation

$$\frac{d}{dt}P_{Z,N}(n,t)=\sum_{Z',N',n'}\lambda(Z,N,n|Z',N',n')\times[P_{Z',N'}(n',t)-P_{Z,N}(n,t)]-[\Lambda^{qf}_{Z,N}(n)+\Lambda^{fis}_{Z,N}(n)]P_{Z,N}(n,t), \qquad (5)$$

where $\Lambda^{qf}_{Z,N}(n)$ and $\Lambda^{fis}_{Z,N}(n)$ are the rates for quasifission in the coordinate R and for fission of heavy nucleus in the DNS with the mass $A_P=Z+N$ of the light nucleus, respectively. Here, $\lambda(Z,N,n|Z',N',n')$ is the rate for the transition from the state $|Z',N',n'\rangle$ to the state $|Z,N,n\rangle$ with $\lambda(Z,N,n|Z',N',n')=\lambda(Z',N',n'|Z,N,n)$. These states are eigenfunctions of H_{in} with the eigenvalues $E_n^{Z,N}$:

$$H_{in}|Z,N,n\rangle=E_n^{Z,N}|Z,N,n\rangle.$$

The transition rate can be expressed in the time-dependent perturbation theory as

$$\begin{aligned}&\lambda(Z,N,n|Z',N',n')\\&=\frac{1}{\Delta t}\left|\langle Z,N,n|\mathcal{T}\exp\left(-\frac{i}{\hbar}\int_t^{t+\Delta t}V^I_{int}(\tau)d\tau\right)|Z',N',n'\rangle\right|^2\\&=\frac{1}{\Delta t}|\langle Z,N,n|V_{int}|Z',N',n'\rangle|^2\\&\quad\times\frac{\sin^2[\Delta t(E_n^{Z,N}-E_{n'}^{Z',N'})/2\hbar]}{(E_n^{Z,N}-E_{n'}^{Z',N'})^2/4}.\end{aligned} \qquad (6)$$

Here, $V^I_{int}(\tau)=\exp(iH_{in}\tau/\hbar)V_{int}\exp(-iH_{in}\tau/\hbar)$ and $\mathcal{T}$ is the time-ordering operator. The time interval $\Delta t=10^{-22}$ s is larger than the relaxation time of the mean field, but considerably smaller than $2\pi\hbar/\Delta E$, where ΔE is the energy spread of the states belonging to one macroscopic cell.

It follows from the single-particle nature of V_{int} that $\lambda(Z,N,n|Z',N',n')$ is nonzero only if the states n and n' differ by one particle-hole pair. The energy difference of the configurations in this case is reduced to the difference of single-particle energies as explained in Refs. [11,23]. The mutual influence of the mean fields of the reaction partners leads to a change of the single-particle energies with respect to those of noninteracting nuclei. Due to the long-range character, the Coulomb interaction gives the main contribution to this energy change. Thus, for the protons we shift the difference between single-particle energies in the following way:

$\epsilon_P - \epsilon_T \to \epsilon_P - \epsilon_T + e^2 Z(Z_{tot} - Z)/(2R_m)$, where Z_{tot} is the total charge number of the DNS. It follows from Eqs. (4) and (6) that

$$\lambda(Z,N,n|Z\pm 1,N,n') = \frac{1}{\Delta t}\sum_{P,T}^{Z} |g_{PT}|^2 n_T^{Z\pm 1,n'}(1-n_P^{Z\pm 1,n'}) n_P^{Z,n}(1-n_T^{Z,n}) \times \frac{\sin^2[\Delta t(\epsilon_P-\epsilon_T)/2\hbar]}{(\epsilon_P-\epsilon_T)^2/4},$$

$$\lambda(Z,N,n|Z,N\pm 1,n') = \frac{1}{\Delta t}\sum_{P,T}^{N} |g_{PT}|^2 n_T^{N\pm 1,n'}(1-n_P^{N\pm 1,n'}) n_P^{N,n}(1-n_T^{N,n}) \times \frac{\sin^2[\Delta t(\epsilon_P-\epsilon_T)/2\hbar]}{(\epsilon_P-\epsilon_T)^2/4}. \quad (7)$$

The quantities with the subindices P and T are the corresponding occupation numbers and single-particle energies in the light and heavier nuclei, respectively. The notation $\Sigma_{P,T}^{Z}$ ($\Sigma_{P,T}^{N}$) means the summation over the proton (neutron) single-particle states of both nuclei of the DNS. Here, $n_P^{Z,n}$ and $n_P^{N,n}$ are the occupation numbers of the proton and neutron single-particle states in the state n in the light nucleus with Z protons and N neutrons, respectively. The occupation numbers are assumed to be zero or unity. The upper and lower subindices P or T correspond to the "+" and "−" signs in Eq. (7), respectively. Since V_{int} in Eq. (4) consists of single-particle operators only, the following restricted sums over the states n, which can be reached from states n', yield unity:

$$\sum_n n_T^{Z(N),n}(1-n_P^{Z(N),n}) = 1,$$

$$\sum_n n_P^{Z(N),n}(1-n_T^{Z(N),n}) = 1.$$

Therefore, summing Eq. (7) over n eliminates the above factors. Assuming that the thermal equilibrium is established in the DNS, we factorize $P_{Z,N}(n,t)$ in the form [11,23]

$$P_{Z,N}(n,t) = P_{Z,N}(t)\Phi_{Z,N}(n,\Theta),$$

where $\Phi_{Z,N}(n,\Theta)$ is the probability of finding the DNS with given Z and N in state n. These probabilities are normalized to unity: $\Sigma_n \Phi_{Z,N}(n,\Theta) = 1$. Then, we assume

$$\sum_n n_T^{Z(N),n}(1-n_P^{Z(N),n})\Phi_{Z,N}(n,\Theta) = n_T^{Z(N)}(\Theta)[1-n_P^{Z(N)}(\Theta)], \quad (8)$$

where $n_P^{Z(N)}(\Theta)$ $[n_T^{Z(N)}(\Theta)]$ are the Fermi occupation numbers of the single-particle proton (neutron) states in the light (heavy) nucleus according to a Fermi distribution as a function of the DNS temperature $\Theta(Z,N)$. Summing Eq. (5) over n, we finally obtain the equations

$$\frac{d}{dt}P_{Z,N}(t) = \Delta_{Z+1,N}^{(-,0)}P_{Z+1,N}(t) + \Delta_{Z-1,N}^{(+,0)}P_{Z-1,N}(t) + \Delta_{Z,N+1}^{(0,-)}P_{Z,N+1}(t) + \Delta_{Z,N-1}^{(0,+)}P_{Z,N-1}(t) - (\Delta_{Z,N}^{(-,0)} + \Delta_{Z,N}^{(+,0)} + \Delta_{Z,N}^{(0,-)} + \Delta_{Z,N}^{(0,+)} + \Lambda_{Z,N}^{qf} + \Lambda_{Z,N}^{fis})P_{Z,N}(t), \quad (9)$$

with initial condition $P_{Z,N}(0) = \delta_{Z,Z_i}\delta_{N,N_i}$ and the transport coefficients

$$\Delta_{Z,N}^{(\pm,0)}(\Theta) = \frac{1}{\Delta t}\sum_{P,T}^{Z} |g_{PT}|^2 n_P^T(\Theta)[1-n_T^P(\Theta)] \times \frac{\sin^2[\Delta t(\epsilon_P-\epsilon_T)/2\hbar]}{(\epsilon_P-\epsilon_T)^2/4},$$

$$\Delta_{Z,N}^{(0,\pm)}(\Theta) = \frac{1}{\Delta t}\sum_{P,T}^{N} |g_{PT}|^2 n_P^T(\Theta)[1-n_T^P(\Theta)] \times \frac{\sin^2[\Delta t(\epsilon_P-\epsilon_T)/2\hbar]}{(\epsilon_P-\epsilon_T)^2/4},$$

$$\Lambda_{Z,N}^{qf}(\Theta) = \sum_n \Lambda_{Z,N}^{qf}(n)\Phi_{Z,N}(n,\Theta),$$

$$\Lambda_{Z,N}^{fis}(\Theta) = \sum_n \Lambda_{Z,N}^{fis}(n)\Phi_{Z,N}(n,\Theta). \quad (10)$$

The rates characterize the proton and neutron transfers from a heavy to a light nucleus ($\Delta_{Z,N}^{(+,0)}, \Delta_{Z,N}^{(0,+)}$) or in opposite direction ($\Delta_{Z,N}^{(-,0)}, \Delta_{Z,N}^{(0,-)}$). Averaging the rates of decay probability in R and of fission of the heavy nucleus over internal states, we get the coefficients $\Lambda_{Z,N}^{qf}(\Theta)$ and $\Lambda_{Z,N}^{fis}(\Theta)$ depending on Θ. The expressions chosen for these rates will be discussed below. The solution of the master equation (9), with the decay term and the microscopically calculated transport coefficients, yields a realistic description of the DNS evolution in charge and mass asymmetries. In Eq. (9), we take only transitions $Z \rightleftharpoons Z \pm 1$ and $N \rightleftharpoons N \pm 1$ into account in the spirit of the independent-particle model.

In order to simplify the calculation of the transport coefficients (10) for each Z and N, we used single-particle levels obtained with spherical Woods-Saxon potentials, spin-orbit and Coulomb interactions [11,24]. Examples of these level schemes are given in Ref. [25]. The energies of the last occupied levels are normalized to describe the nucleon separation energies known from the experiment or self-consistent calculations [11,24]. As was shown in [17,24], this simplified procedure takes the peculiarities of the structure of the DNS nuclei effectively into account. Indeed, the values of $\Delta_{Z,N}^{(\pm,0)}$ and $\Delta_{Z,N}^{(0,\pm)}$ depend on sums over single-particle states which is not crucial for the level splitting due

to deformation. The nucleon transfer mainly occurs between the single-particle states near the Fermi levels of the DNS nuclei due to the action of the Pauli blocking factors $n_{T_P}(1-n_{P_T})$ and the selection rules in the matrix elements g_{PT}. For the calculation of the matrix elements g_{PT} we used the analytical method given in Ref. [26]. We did not fit any parameters, they were taken the same for all reactions considered.

If at some Z and N, the rates $\Delta_{Z,N}^{(+,0)}$ and $\Delta_{Z,N}^{(0,+)}$ are close to $\Delta_{Z,N}^{(-,0)}$ and $\Delta_{Z,N}^{(0,-)}$, respectively, and the inequalities $\Delta_{Z,N}^{(+,0)} > \Delta_{Z,N}^{(-,0)}$ and $\Delta_{Z,N}^{(+,0)} < \Delta_{Z,N}^{(-,0)}$ ($\Delta_{Z,N}^{(0,+)} > \Delta_{Z,N}^{(0,-)}$ and $\Delta_{Z,N}^{(0,+)} < \Delta_{Z,N}^{(0,-)}$) hold for smaller and larger Z (N), respectively, or $\Delta_{Z,N}^{(\pm,0)}$ and $\Delta_{Z,N}^{(0,\pm)}$ are minimal with respect to those for neighboring Z and N, the distribution $P_{Z,N}$ may have a maximum in accordance with Eqs. (9).

In our treatment, the effects of deformation are effectively taken into account in Eqs. (9) through the dependence of the excitation energy E^* or Θ of the DNS on Z, N, and deformations of the DNS nuclei. The change of E^* is opposite in sign to the change of the DNS potential energy which is discussed below.

The rotational energy of the DNS is defined as

$$V_{rot}(R,Z,N,\beta_P,\beta_T,J)=\frac{\hbar^2 J(J+1)}{2(\Im_P+\Im_T+\mu_{PT}R^2)}, \quad (11)$$

where $\Im_P$ and $\Im_T$ are the moments of inertia of the DNS nuclei, $\mu_{PT}=mA_PA_T/A$, and β_P and β_T the deformation parameters of the DNS nuclei. In order to take the DNS rotation phenomenologically into consideration in Eq. (10), one can renormalize ϵ_P and ϵ_T as

$$\epsilon_P \to \epsilon_P + \frac{\Im_P+\mu_{PT}R^2A_T/A}{A_P(\Im_P+\Im_T+\mu_{PT}R^2)}V_{rot},$$

$$\epsilon_T \to \epsilon_T + \frac{\Im_T+\mu_{PT}R^2A_P/A}{A_T(\Im_P+\Im_T+\mu_{PT}R^2)}V_{rot}, \quad (12)$$

i.e., the rotational energy is distributed between the DNS nuclei proportionally to their moments of inertia with respect to the center of mass of the DNS. It will be shown below that the dependence of our results on angular momentum is rather weak.

B. Potential energy of the DNS

The DNS potential energy is calculated as in Refs. [13,17],

$$U(R,Z,N,\beta_P,\beta_T,J)=B_P(\beta_P^{gs})+B_T(\beta_T^{gs})+B_{def}(\beta_P,\beta_T)+V(R,Z,N,\beta_P,\beta_T,J), \quad (13)$$

where B_P and B_T are the mass excesses [27,28] of the fragments at their ground states (g.s.) with deformation parameters β_P^{gs} and β_T^{gs}, and B_{def} the energy of the deformation of the DNS nuclei with $B_{def}(\beta_P^{gs},\beta_T^{gs})=0$. The nucleus-nucleus potential [13,17] in Eq. (13),

$$V(R,Z,N,\beta_P,\beta_T,J)=V_C(R,Z,\beta_P,\beta_T)+V_N(R,Z,N,\beta_P,\beta_T)+V_{rot}(R,Z,N,\beta_P,\beta_T,J), \quad (14)$$

is the sum of the centrifugal potential V_{rot}, the Coulomb potential V_C, and the nuclear potential V_N. For the nuclear part of V, we use a double folding formalism with the effective density-dependent nucleon-nucleon interaction [13] which is known from the theory of finite Fermi systems. As a result of various calculations, the simple approximate expression is obtained:

$$V_N(R,Z,N,\beta_P,\beta_T)=V_0\{\exp[-2(R-R_{PT})\alpha/R_{PT}]-2\exp[-(R-R_{PT})\alpha/R_{PT}]\}, \quad (15)$$

$$V_0=2\pi a_P a_T \bar{R}(11.3-0.82\bar{R}_0)\times\left(1+\frac{0.16(\beta_P+\beta_T)}{1+\exp[-17(|\eta|-0.5)]}\right),$$

$$\alpha=(11.47-17.32a_Pa_T+2.07\bar{R}_0)[1+0.25(\beta_P+\beta_T)],$$

$$\bar{R}_0=R_PR_T/(R_P+R_T), \quad R_{PT}=D_P+D_T+0.1 \text{ fm},$$

$$D_{P(T)}=R_{P(T)}\left[1+\left(\frac{5}{4\pi}\right)^{1/2}\beta_{P(T)}-\frac{1}{4\pi}\beta_{P(T)}^2\right],$$

$$\bar{R}=\bar{R}_P\bar{R}_T/(\bar{R}_P+\bar{R}_T),$$

$$\bar{R}_{P(T)}=D_{P(T)}\frac{1+\left(\frac{5}{4\pi}\right)^{1/2}\beta_{P(T)}-\frac{1}{4\pi}\beta_{P(T)}^2}{1+4\left(\frac{5}{4\pi}\right)^{1/2}\beta_{P(T)}-\frac{1}{4\pi}\beta_{P(T)}^2}.$$

Here, $a_T=0.56$ fm and $a_P=a_T-0.015|\eta|$ are the diffusenesses of the DNS heavy and light nuclei, respectively (light nucleus has small diffuseness), and $R_{P(T)}=r_0A_{P(T)}^{1/3}$ ($r_0=1.16$ fm) is the radius of nucleus "P" ("T"). Deformed nuclei are treated in the pole-to-pole orientation.

C. Decay rate of the DNS

The decaying DNS has to overcome the potential barrier B_{qf} [13]. The value of B_{qf} coincides with the depth of the pocket in the nucleus-nucleus potential which is situated at the distance $R_m=R_P[1+\beta_P\sqrt{5/(4\pi)}]+R_T[1+\beta_T\sqrt{5/(4\pi)}]+0.5$ fm and keeps the DNS nuclei in contact [13,14,16]. The values of B_{qf}, depending on Z, mainly determine the lifetime t_0 of the DNS. Since we consider reactions with heavy nuclei which occur slightly above the Coulomb barrier, which is at $R_b \approx R_P[1+\beta_P\sqrt{5/(4\pi)}]+R_T[1+\beta_T\sqrt{5/(4\pi)}]+2$ fm, the quasifission barrier B_{qf} depends weakly on angular momentum for $J<70$ because the DNS has a large moment of inertia.

Thus, the value of B_{qf} is calculated with Eq. (14). In the considered heavy DNS, B_{qf} is about 4.5 MeV at $Z=20$ and less than 0.5 MeV for $Z=Z_{tot}/2\pm 10$. From a qualitative point of view it is clear that in the approaching or disintegrating stage of two nuclei, the barrier appears because the nuclear forces become smaller than the Coulomb forces outside some distance. For the asymmetric DNS, a large value of B_{qf} is evident because $R_b > R_m$ and the Q value in fusion channel is positive. For the nearly symmetric DNS considered, the quasifission barrier resulting from our calculations is consistent with the existence of a reflection-asymmetric third minima found experimentally [29] in some heavy nuclei, and with the shell model and macroscopic-microscopic calculations [30]. It was earlier mentioned in Ref. [31] that the qualitative reason for such a third well is the complete formation of the fragments at the scission point. Indeed, a nucleus in the third minimum is similar to a DNS which is kept against the decay by the barrier. Our calculations of the potential energy of touching (scission-point) configurations are more appropriate than the liquid drop calculations for the fission in which various phenomenological criteria of scission are used instead of the dynamical treatment of the scission stage and of the transition to separate nuclei with different N/Z ratios.

In Eq. (14), only the neck degree of freedom is assumed to be frozen. Within the two-center shell model [19] the DNS has a neck parameter $\varepsilon \approx 0.8$, which corresponds to the neck formed due to the overlap of the diffused tails of two nuclei. In Ref. [19], we found that the neck size remains practically constant during the time of fusion or quasifission, since we obtained very large inertia in the microscopical treatment. In the calculations with the two-center shell model, the quasifission barrier exists even for a large neck size, and the appearance of this barrier is not related to the frozen neck in Eq. (14).

The decay of the DNS in R can be treated with the one-dimensional Kramers rate [32–34] $\Lambda^{qf}_{Z,N}(\Theta)$,

$$\Lambda^{qf}_{Z,N}(\Theta) = \frac{\omega}{2\pi\omega^{B_{qf}}}\left(\sqrt{\left(\frac{\Gamma}{2\hbar}\right)^2 + (\omega^{B_{qf}})^2} - \frac{\Gamma}{2\hbar}\right) \times \exp\left(-\frac{B_{qf}(Z,N)}{\Theta(Z,N)}\right), \tag{16}$$

which exponentially depends on the quasifission barrier $B_{qf}(Z,N)$ for a given charge and mass asymmetry [13]. The height B_{qf} of this barrier uniformly decreases with increasing Z up to the symmetric DNS because the increasing Coulomb repulsion leads to very shallow pockets in the nucleus-nucleus potential for near symmetric configurations. The temperature $\Theta(Z,N)$ is calculated by using the Fermi-gas expression $\Theta=\sqrt{E^*/a}$ with the excitation energy $E^*(Z,N)$ of the DNS and with the level-density parameter $a = A_{tot}/12$ MeV^{-1}. If the fusion barrier in the Z coordinate is located at $Z=Z_{BG}$ (Businaro-Gallone point, N_{BG} is chosen from the minimization of the potential energy with respect to N at fixed $Z=Z_{BG}$), the excitation energy $E^*(Z,N)$ of the DNS increases with decreasing Z for $Z<Z_{BG}$ and with increasing Z for $Z>Z_{BG}$. The calculated DNS potential energy surfaces as a function of Z have fusion barriers at $Z_{BG} = 8-12$ in the cold and hot fusion reactions considered. In Eq. (16), the frequency $\omega^{B_{qf}}$ of the inverted harmonic oscillator approximates the potential V in R around the top of the quasifission barrier, and ω is the frequency of the harmonic oscillator approximating the potential in R at the bottom of the pocket. Here, we can use constant values $\hbar\omega^{B_{qf}} = 1.0$ MeV and $\hbar\omega = 2.0$ MeV [35] for the reactions considered in the following. Further, we set the width $\Gamma = 2.8$ MeV in Eq. (16) which means that the friction coefficient in R has the same order of magnitude as the one calculated within the one-body dissipation models [9,13]. The possibility to apply the Kramers expression to relatively small barriers was demonstrated in Ref. [36]. The transient times are quite short for the considered excitation energies E^* and quasifission barriers B_{qf} and, therefore, the use of expression (16) is justified. As in fission where more channels are involved, the Kramers formula is suitable here within the accuracy of the calculation of the potential barriers.

The diffusion in mass asymmetry is quite fast and the temperature Θ for a nearly symmetric DNS is about 1.5 MeV in the reactions considered. Therefore, we find $\exp(-B_{qf}/\Theta)\approx 0.7$ in Eq. (16) for a quasifission barrier of 0.5 MeV and the calculated yields of nearly symmetric products are not crucial to the value of B_{qf} in the interval 0–0.8 MeV for $Z=Z_{tot}/2\pm 10$.

D. Charge and mass yields for quasifission

The measurable charge and mass yields for quasifission can be expressed by the product of the formation probability $P_{Z,N}(t)$ of the DNS configuration with charge and mass asymmetries given by Z and N, and of the decay probability in R represented by the quasifission rate $\Lambda^{qf}_{Z,N}$:

$$Y_{Z,N}(t_0) = \Lambda^{qf}_{Z,N}\int_0^{t_0} P_{Z,N}(t)\,dt. \tag{17}$$

Here, t_0 is the time of reaction which is determined by solving the equation

$$\sum_{Z,N}\left[\Lambda^{qf}_{Z,N} + \Lambda^{fis}_{Z_{tot}-Z,N_{tot}-N}\right]\int_0^{t_0} P_{Z,N}(t)\,dt = 1 - P_{CN},$$

where $N_{tot}=A_{tot}-Z_{tot}$ and $P_{CN}=\Sigma_{Z<Z_{BG},N<N_{BG}}P_{Z,N}(t_0)$ is the fusion probability, defined by the fraction of probability existing at time t_0 for $Z<Z_{BG}$ and $N<N_{BG}$. With this definition, the calculated values of P_{CN} practically coincide with those obtained in Ref. [14] with another method. Mainly, the decay of the DNS with $Z>Z_{BG}$ contributes to the quasifission yield. The DNS with $Z<Z_{BG}$ are assumed to evolve to the compound nucleus with a high probability. In general, the characteristic time (a few units of 10^{-21} s) of this evolution is shorter than the decay time of the unstable superheavy compound nucleus or unstable superheavy nucleus in the very asymmetric DNS.

The mass yield of quasifission products is defined as follows:

$$Y(A_P) = \sum_Z Y_{Z,A_P-Z}(t_0). \tag{18}$$

For the energies above the Coulomb barrier V_b, the capture cross section is estimated as

$$\sigma_{cap}(E_{\rm c.m.})=\frac{\pi\hbar^2}{2\mu E_{\rm c.m.}}J_{cap}(J_{cap}+1), \tag{19}$$

where $\hbar J_{cap}\leqslant\sqrt{2\mu R_b^2(E_{\rm c.m.}-V_b)}$ and must be smaller than the critical angular momentum J_{crit}. The trajectories with $J\geqslant J_{crit}$ contribute to deep-inelastic collisions. In the DNS model [13,14,16], the total quasifission cross section

$$\sigma_{qf}(E_{\rm c.m.})\approx[1-P_{CN}(E_{\rm c.m.})-P_f(E_{\rm c.m.})]\sigma_{cap}(E_{\rm c.m.}) \tag{20}$$

depends on the capture cross section σ_{cap} for the transition of the colliding nuclei over the entrance (Coulomb) barrier and on the probability P_{CN} of the compound nucleus formation after the capture. Here, $P_f=\Sigma_{Z,N}\Lambda^{fis}_{Z_{tot}-Z,N_{tot}-N}\int_0^{t_0}P_{Z,N}(t)dt$. In the DNS model, the projectile is captured by the target and a DNS is formed, which either evolves into the compound nucleus or decays by quasifission. Since in this paper we are mainly interested in reactions with heavy ions which occur near the Coulomb barrier and have quite small values of P_{CN}, only partial waves with angular momenta J less than the critical angular momentum contribute to σ_{qf}, and $\sigma_{qf}\approx\sigma_{cap}$ seems to be a good approximation. Larger values of J contributing to deep-inelastic collisions are not treated here. The total quasifission cross section $\sigma_{qf}(E_{\rm c.m.})=\Sigma_{A_P}\sigma_{qf}(E_{\rm c.m.},A_P)$ can be split into the cross sections $\sigma_{qf}(E_{\rm c.m.},A_P)$ of the quasifission products with certain mass numbers A_P of the light fragment. The cross section of the yield of quasifission products with mass A_P is thus defined as

$$\sigma_{qf}(E_{\rm c.m.},A_P)=Y(A_P)\sigma_{cap}(E_{\rm c.m.}) \tag{21}$$

with $\Sigma_{A_P}Y(A_P)=1-P_{CN}(E_{\rm c.m.})-P_f(E_{\rm c.m.})$.

E. Total kinetic energy distribution

In order to calculate the average total kinetic energy (TKE) of the quasifission products and its dispersion, one has to regard the deformation of the fragments in addition. Calculating the nucleus-nucleus potential with Eq. (14) and the binding energies with the two-center shell model, we found that the equilibrium deformations of the DNS nuclei deviate from their values in the ground states due to polarization effects. The polarization is quite strong for nearly symmetric DNS because of the strong Coulomb interaction [37]. For the nuclei with $A=A_{tot}/2\pm 20$ in the DNS, we found deformations which are about three to four times larger than the deformations of the nuclei in their ground states. These large deformations of the DNS nuclei have to be considered to explain the experimental data of the TKE of the quasifission fragments. However, the increase of B_{def} in Eq. (13) with $\beta_P-\beta_P^{gs}$ and $\beta_T-\beta_T^{gs}$ is compensated within 0.5–3 MeV by the decrease of the nucleus-nucleus interaction. Therefore, for $\beta_P>\beta_P^{gs}$ and $\beta_T>\beta_T^{gs}$ the DNS potential energy as a function of Z and N at $R=R_m$ (driving potential) weakly depends on the deformation parameters and $U(R_m,Z,N,\beta_P,\beta_T,J)\approx U(R_m,Z,N,\beta_P^{gs},\beta_T^{gs},J)$. The same can be concluded from the calculations within the scission-point model [38].

The distribution of the fragments in charge, mass, and deformation can be written as

$$\begin{aligned}W&=W(Z,N,\beta_P,\beta_T)\\&=Y_{Z,N}(t_0)w_{\beta_P}(Z,N)w_{\beta_T}(Z_{tot}-Z,N_{tot}-N).\end{aligned} \tag{22}$$

Here, $w_\beta(Z,N)$ is taken as a Gaussian probability distribution in deformation at fixed values of Z and N:

$$w_\beta(Z,N)=\frac{1}{\sqrt{2\pi\sigma_\beta^2}}\exp[-(\beta-\langle\beta\rangle)^2/(2\sigma_\beta^2)], \tag{23}$$

with $\sigma_\beta^2=[\hbar\omega_{vib}/(2C_{vib})]\coth[\hbar\omega_{vib}/(2k\Theta)]$, where $\omega_{vib}(Z,N)$ and $C_{vib}(Z,N)$ are the frequency and stiffness parameter of quadrupole vibrations, respectively. The stiffness parameter is determined as [39]

$$C_{vib}(Z,N)=\frac{\hbar\omega_{vib}[3Zr_0^2(Z+N)^{2/3}/(4\pi)]^2}{2B(E2)_{vib}}. \tag{24}$$

Since not in all nuclei the first vibrational levels are well defined, we take 2^+ states presented in Ref. [40] as vibrational ones if $B(E2)^{exp}<0.55\ e^2\,{\rm b}^2$. If $B(E2)^{exp}>0.55\ e^2\,{\rm b}^2$, the 2^+ states with the energy $E_{2^+}^{exp}$ presented in Ref. [40] are considered as rotational ones. In this case $\hbar\omega_{vib}$ and $B(E2)_{vib}$ can be estimated as $\hbar\omega_{vib}\approx E_{2^+}^{exp}B(E2)^{exp}/0.55\ e^2\,{\rm b}^2$ and $B(E2)_{vib}\approx E_{2^+}^{exp}B(E2)^{exp}/(\hbar\omega_{vib})=0.55\ e^2\,{\rm b}^2$. For known vibrational states in nuclei with $\hbar\omega_{vib}>E_{2^+}$, this estimation seems to be quite good. Since $\langle\beta\rangle$ is larger than the β value in the ground state because of the polarization effects, we assume here that the β vibration around $\langle\beta\rangle$ has the same properties as the β vibration near the ground state.

Applying distribution (22) we calculate the average total kinetic energy as a function of the mass number $A_P=Z+N$ of the light fragment:

$$\begin{aligned}\langle{\rm TKE}(A_P)\rangle&=\int\int d\beta_P d\beta_T\sum_{\substack{Z,N\\Z+N=A_P}}{\rm TKE}\cdot W\Big/\left(\int\int d\beta_P d\beta_T\sum_{\substack{Z,N\\Z+N=A_P}}W\right)\\&\approx\sum_Z{\rm TKE}|_{\substack{\beta_P=\langle\beta_P\rangle\\\beta_T=\langle\beta_T\rangle}}Y_{Z,A_P-Z}(t_0)\Big/\sum_Z Y_{Z,A_P-Z}(t_0),\end{aligned} \tag{25}$$

with $\mathrm{TKE}=V_{nucl}(R_b)+V_{Coul}(R_b)$, where the radius $R_b=R_b(Z,N,\beta_P,\beta_T)$ is the position of the Coulomb barrier.

The variance of TKE can be written as a sum of the contributions of variances of the exchange of nucleons and of the deformations:

$$\sigma^2_{\mathrm{TKE}}(A_P)\approx\sum_Z \mathrm{TKE}^2\big|_{\substack{\beta_P=\langle\beta_P\rangle\\ \beta_T=\langle\beta_T\rangle}} Y_{Z,A_P-Z}(t_0)\Big/\sum_Z Y_{Z,A_P-Z}(t_0)-\langle TKE(A_P)\rangle^2+[\sigma^{def}_{TKE}(A_P)]^2_{\text{light nucleus ``}P\text{''}}$$
$$+[\sigma^{def}_{TKE}(A_P)]^2_{\text{heavy nucleus ``}T\text{''}}, \tag{26}$$

where

$$[\sigma^{def}_{TKE}(A_P)]^2_j=\sum_Z\left(\frac{\partial\mathrm{TKE}}{\partial\beta_j}\right)^2\Big|_{\substack{\beta_P=\langle\beta_P\rangle\\ \beta_T=\langle\beta_T\rangle}}\sigma^2_{\beta_j}Y_{Z,A_P-Z}(t_0)\Big/\sum_Z Y_{Z,A_P-Z}(t_0) \tag{27}$$

with $j=$ ``$P$'' or ``T.''

III. RESULTS AND DISCUSSION

The decay rate of the DNS is calculated by using the value of $B_{qf}(Z,N)$ determined with potential (14). The decrease of B_{qf} with increasing Z was demonstrated in Ref. [16]. In all reactions considered here, the lifetime t_0 of the DNS is about $(3-4)\times10^{-20}$ s, which is in agreement with the time extracted from experimental data [41]. The presence of $\Lambda^{qf}_{Z,N}\neq0$ in Eq. (9) decreases the yield of symmetric DNS. Thus, this decay term is very important for the correct description of the yield of quasifission products which are formed during the reaction time t_0. This time is at least ten times larger than the characteristic time of deep inelastic collisions.

The calculated mean values of the TKE for the products of nearly symmetric quasifission in all reactions considered follow the experimental Viola systematic: $\langle\mathrm{TKE}\rangle=0.131Z^2_{tot}/A^{1/3}_{tot}$ [42]. This systematic is close to the experimental one $\langle\mathrm{TKE}\rangle=0.133\,23Z^2_{tot}/A^{1/3}_{tot}-11.64$ given in Ref. [43] for nuclei in the mass region $230\leqslant A_{tot}<256$. It should be mentioned that the experimental determination of the TKE has large systematic and statistical uncertainties. For example, for $A_P=A_{tot}/2\pm20$ in the $^{48}\mathrm{Ca}+^{238}\mathrm{U}$ reaction, Refs. [6] and [5] give $\langle\mathrm{TKE}\rangle=246\pm4$ MeV and 237 ± 4 MeV, respectively. The calculated $\langle\mathrm{TKE}\rangle$ is 248 MeV and close to the results 249 MeV of Ref. [42] and of 242 MeV of Ref. [43].

A. Hot fusion reactions

1. Reactions with ^{48}Ca beam

The quasifission barrier increases for Z values smaller than the atomic number of projectile, which hinders the decay of asymmetric DNS. However, as is shown in Fig. 1 for the $^{48}\mathrm{Ca}+^{244}\mathrm{Pu}\rightarrow^{292}114$ fusion reaction [21,22], also small yields of nuclei down to Ne can be seen in the quasifission distribution which are presently possible to measure. The measurement of the products with $A_P\approx20$ and 28 in collisions near the Coulomb barrier would confirm the evolution of the DNS to the compound nucleus in the mass asymmetry coordinate. The yield of light products is known to be larger for larger beam energies. In Fig. 1, the value of excitation energy E^*_{CN} of the corresponding compound nucleus is related to the bombarding energy $E_{\mathrm{c.m.}}=E^*_{CN}-Q$, which exceeds the Coulomb barrier by the value

$$E^*_{CN}-[U(Z=20,N=28)+B_{qf}(Z=20,N=28)]$$
$$=E^*(Z_i,N_i)-B_{qf}(Z=20,N=28),$$

where Z_i and N_i are the initial values.

Figure 2 shows the mass yield $Y(A_P)$ and the variance of the TKE of the fragments as functions of the mass number of the light fragment for the hot fusion reaction $^{48}\mathrm{Ca}+^{238}\mathrm{U}\rightarrow^{286}112$ in comparison with experimental data [1,6]. It should be noted that the small oscillations in experimental data are comparable with accuracy of the measurements [1].

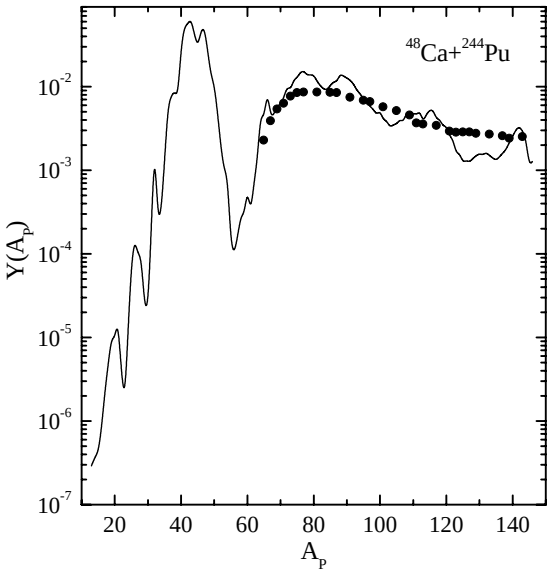

FIG. 1. Mass yield of the quasifission products as a function of the mass number of the light fragment for the hot fusion reaction $^{48}\mathrm{Ca}+^{244}\mathrm{Pu}\rightarrow^{292}114$ at a bombarding energy corresponding to an excitation energy of the compound nucleus of 42 MeV. The available experimental data [1] are shown by solid points.

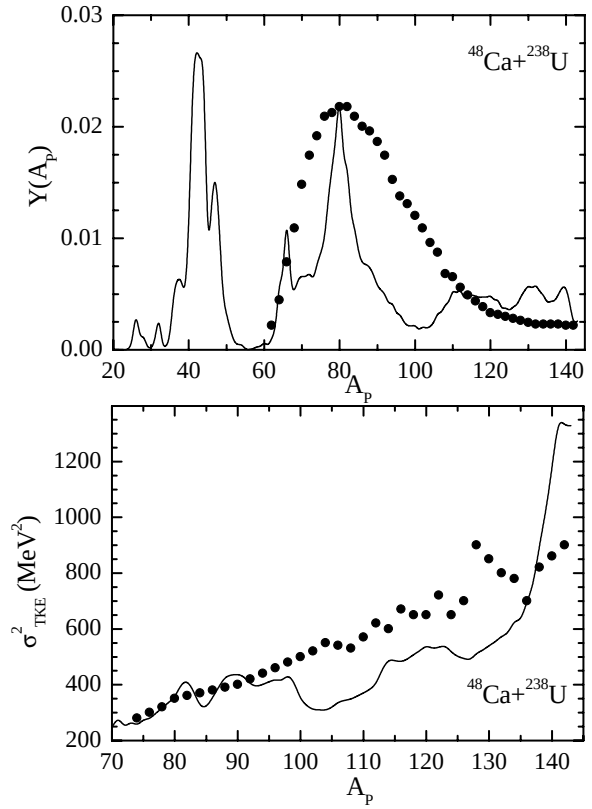

FIG. 2. The calculated (solid lines) mass yield (upper part) and variance of the TKE (lower part) of the quasifission products as a function of the mass number of the light fragment for the hot fusion reaction ^{48}Ca+^{238}U$\rightarrow^{286}$112 at a bombarding energy corresponding to an excitation energy of the compound nucleus of 33.4 MeV. The experimental data [1] are shown by solid points.

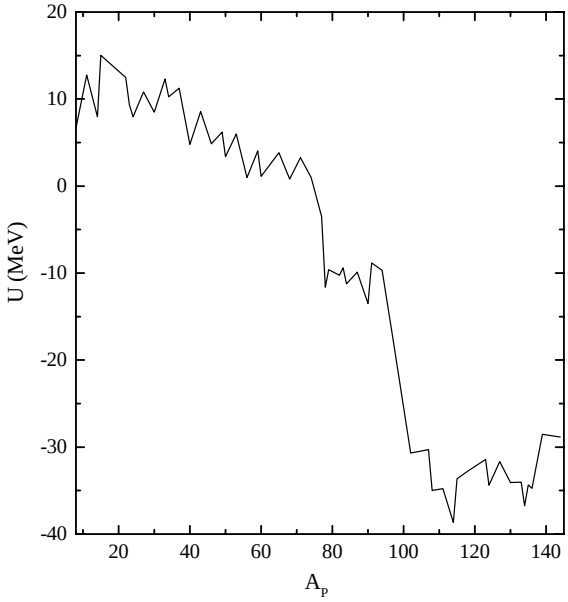

FIG. 3. Calculated dependence of the potential energy of the DNS as a function of the mass number of the light fragment for the ^{48}Ca+^{238}U reaction at $J=0$. The deformation parameters are taken from Ref. [40] for the nuclei of the DNS. The potential energy is minimized with respect to the N/Z ratio, $A_P=Z+N$.

As was experimentally found in Ref. [44], near the initial masses the maximum of mass distribution near $A_P=A_i=48$ is slightly shifted towards smaller $A_P=42-44$, while the maximum of charge distribution corresponds to $Z=Z_i=20$. The same is obtained in our calculations. We note that near the initial masses, the quasifission events overlap with the products of deep-inelastic collisions and were taken out in the experimental analysis, since they are difficult to discriminate from the deep-inelastic events. Since the calculations were performed with angular momenta less than the critical angular momentum and deep-inelastic or quasielastic collisions were not considered, the calculated peak near the initial masses corresponds to quasifission only. The quasifission barriers are rather small in the entrance channel of the reactions considered. If the quasifission barrier for the initial mass asymmetry would be larger, this peak would not be so pronounced and could even vanish.

Maxima in the mass and charge yields arise from minima in the driving potential $U(R_m,Z,N,\beta_P^{gs},\beta_T^{gs},J=0)$ (see Fig. 3) and are caused by shell effects in the dinuclear system. In Fig. 3, we present the driving potential as a function of A_P after minimization of U with respect to the N/Z ratio at each A_P. In comparison to our previous calculations of the mass yield of the quasifission products [16], where only the DNS evolution in Z was treated and N strictly followed Z, the present results reveal more structure. For $A_P>48$, the maximum yield of the quasifission fragments occurs around the nucleus ^{208}Pb for the heavy fragment where the DNS potential energy has a minimum [17]. Together with the decay term in Eq. (9) the evolution of the DNS is hindered to go to smaller mass asymmetry and, correspondingly, the decay probability from the configuration with ^{208}Pb is increased. In the reaction ^{48}Ca+^{238}U (^{48}Ca+^{244}Pu), the height of the peak around $A_P=80$ is 4.5 (3.5) times larger than the height of peaks in the symmetric mass region.

The minima in the dependence of σ^2_{TKE} on A_P are related to stiff nuclei in the DNS such as Zr, Sn, and Pb. In the DNS with soft nuclei, larger values of $(\sigma^{def}_{TKE})^2$ contribute to the maxima in $\sigma^2_{TKE}(A_P)$. Considering the fluctuations of the DNS charge asymmetry (the fluctuations due to the Coulomb interaction) at the fixed mass asymmetry, the fluctuations of the quadrupole deformation parameters of the DNS nuclei, and the fluctuations of the bending mode in the DNS, it is possible to explain the large variance of the TKE distribution as a function of the mass numbers of the fragments.

The calculated data in Fig. 2 are related to the primary (before neutron emission) fragments. Therefore, the maxima and minima in the calculated functions $Y(A_P)$ and $\sigma^2_{TKE}(A_P)$ are more pronounced. The postneutron evaporation washes out some peculiarities of these functions. Taking into account the experimental uncertainties in the identification of quasifission and fusion-fission products (for the calculated ratio between the quasifission and fusion-fission see Table I), and the measurement of mass and energy [1,6], the agreement between the calculated and experimental data is quite good. In the experiment besides the quasifission and fusion-fission, the fission of the heavy nucleus in the DNS with a following

TABLE I. The calculated average variances σ^2_{TKE} of the TKE for the nearly symmetric quasifission products with $A_{tot}/2-20 \leqslant A_P \leqslant A_{tot}/2$, fraction $P_{CN}/\Sigma^{A_{tot}/2}_{A_P=A_{tot}/2-20} Y(A_P)$ of the fusion-fission events with respect to the quasifission events in the mass region $A_{tot}/2-20 \leqslant A_P \leqslant A_{tot}/2$, the calculated average total numbers of emitted neutrons for nearly symmetric quasifission splitting ($\langle M_n^{tot-sym} \rangle$) with $A_{tot}/2-20 \leqslant A_P \leqslant A_{tot}/2$ and for the quasifission splitting ($\langle M_n^{tot-asym} \rangle$) with $A_P < A_{tot}/2-20$. The reactions and the energies of corresponding compound nuclei are indicated.

Reactions	Z_1Z_2	E^*_{CN} (MeV)	σ^2_{TKE} (MeV^2)	$P_{CN}/\Sigma^{A_{tot}/2}_{A_P=A_{tot}/2-20} Y(A_P)$	$\langle M_n^{tot-sym} \rangle$	$\langle M_n^{tot-asym} \rangle$
^{40}Ar+^{165}Ho	1206	89	119	1.1	5.5	3.7
		120	143	0.7	7.3	5.0
^{56}Fe+^{132}Xe	1404	105	348	9.4×10^{-2}	5.7	3.0
		120	379	1.3×10^{-1}	6.5	3.4
^{48}Ca+^{238}U	1840	33.4	756	5.8×10^{-2}	7.0	5.4
		50	840	2.4×10^{-1}	8.1	6.4
^{48}Ca+^{237}Np	1860	33.2	728	2.5×10^{-2}	6.5	4.9
		50	812	1.6×10^{-1}	7.7	6.1
^{48}Ca+^{244}Pu	1880	34.8	805	1.4×10^{-2}	7.5	5.4
		42	846	4.3×10^{-2}	8.2	6.2
		50	893	1.1×10^{-1}	8.5	6.4
^{48}Ca+^{243}Am	1900	33.7	807	6.0×10^{-3}	7.4	5.2
		50	893	3.3×10^{-2}	8.4	6.3
^{48}Ca+^{248}Cm	1920	37	889	4.0×10^{-3}	8.2	5.9
		50	949	1.0×10^{-2}	9.2	6.9
^{48}Ca+^{247}Bk	1940	32.4	865	1.5×10^{-3}	8.0	5.6
		50	933	9.7×10^{-3}	9.1	6.7
^{48}Ca+^{249}Cf	1960	30.6	808	1.3×10^{-3}	7.7	5.4
		50	949	3.2×10^{-2}	9.0	6.8
^{50}Ti+^{248}Cm	2112	50	932	8.5×10^{-3}	9.0	6.8
^{54}Cr+^{248}Cm	2304	50	995	3.8×10^{-4}	9.4	7.2
^{64}Ni+^{244}Pu	2632	50	1021	9.5×10^{-6}	10.0	7.8
^{64}Ni+^{248}Cm	2688	50	1073	7.0×10^{-6}	10.4	8.2
^{58}Fe+^{208}Pb	2132	14.5	420	4.9×10^{-5}	3.5	2.1
		30	484	5.9×10^{-2}	4.8	3.2
^{58}Fe+^{232}Th	2340	53	878	6.2×10^{-4}	8.3	6.2
^{58}Fe+^{244}Pu	2444	44	941	5.7×10^{-5}	8.9	6.7
		50	971	2.4×10^{-4}	9.4	7.3
^{58}Fe+^{248}Cm	2496	33	900	7.0×10^{-6}	8.3	6.2
		50	984	6.1×10^{-5}	9.7	7.4
^{58}Fe+^{249}Cf	2548	33	841	6.2×10^{-6}	8.3	5.9
		50	918	6.9×10^{-5}	9.6	7.4
^{64}Ni+^{208}Pb	2296	12.5	499	1.2×10^{-5}	3.5	2.1
		20	549	1.8×10^{-3}	4.1	2.8
		30	609	8.5×10^{-3}	4.9	3.5
^{70}Ni+^{208}Pb	2296	20	565	4.2×10^{-5}	4.8	2.8
		30	625	3.5×10^{-4}	5.6	3.4
^{86}Kr+^{198}Pt	2808	25	692	4.0×10^{-7}	4.8	2.8
		50	827	3.2×10^{-5}	8.2	5.5
^{86}Kr+^{208}Pb	2952	17	738	2.1×10^{-7}	4.8	2.8
		30	813	2.0×10^{-5}	7.0	4.7

fusion of one of the fission fragments with the light nucleus of the DNS and ternary processes with the emission of a light particle are identified as two-body processes of complete momentum transfer.

For the ^{48}Ca+^{248}Cm reaction, the calculated data of $Y(A_P)$ and $\sigma^2_{TKE}(A_P)$ are compared with the experimental data in Fig. 4. Since the DNS has a large moment of inertia, the data calculated for $J=0$ and 70 are very similar. Therefore, the dependence of $Y(A_P)$ and $\sigma^2_{TKE}(A_P)$ on angular momentum is rather weak that confirms the applicability of Eqs. (20) and (21). For $A_P > 100$, $[\sigma^{def}_{TKE}(A_P)]^2$ mainly contributes to $\sigma^2_{TKE}(A_P)$ (Fig. 5); the same is for all the reac-

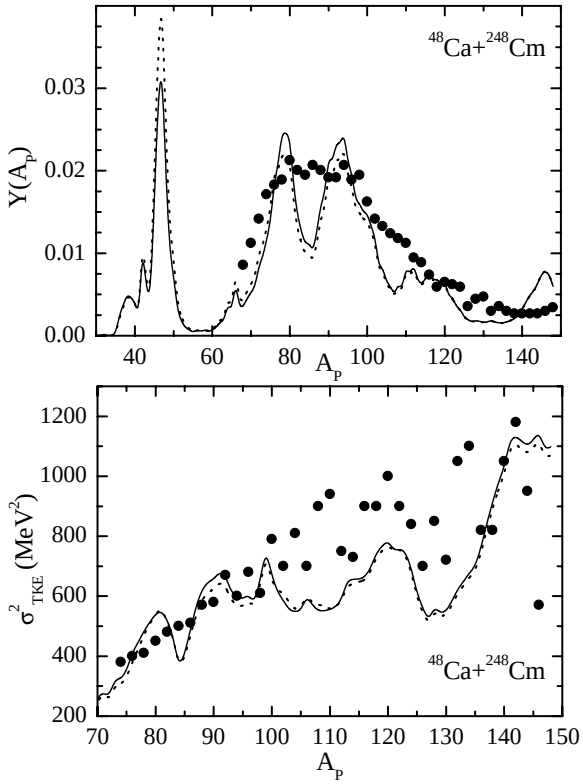

FIG. 4. The same as in Fig. 2, but for the hot fusion reaction ^{48}Ca+^{248}Cm$\rightarrow^{296}$116 at the bombarding energy corresponding to an excitation energy of the compound nucleus of 37 MeV. The results calculated for $J=0$ and 70 are presented by solid and dotted curves, respectively.

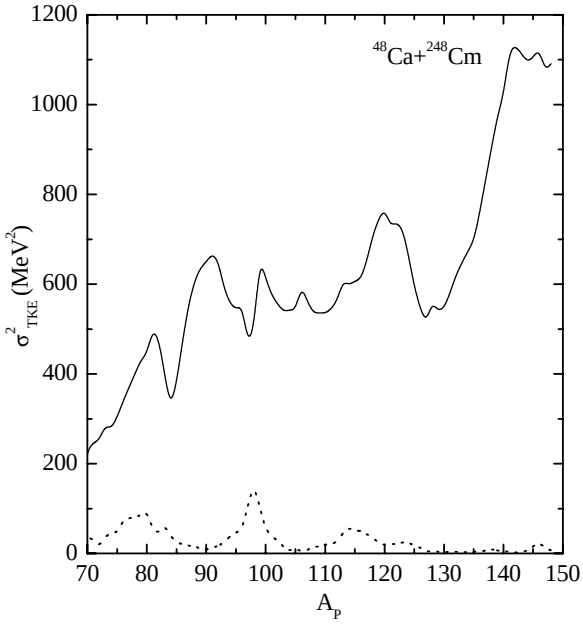

FIG. 5. The fluctuations in deformation (solid line) and in nucleon exchange (dotted line) to the variance of the TKE of quasifission products as a function of the mass number of the light fragment for the hot fusion reaction ^{48}Ca+^{248}Cm at a bombarding energy corresponding to an excitation energy of the compound nucleus of 37 MeV.

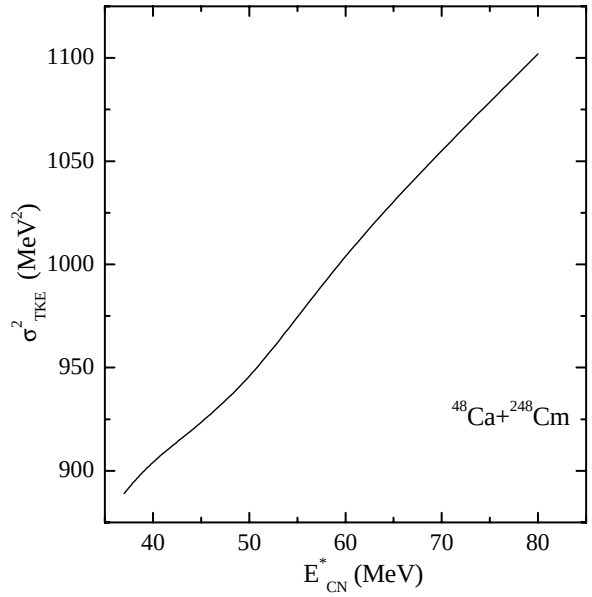

FIG. 6. Calculated variance of the TKE of quasifission products as a function of the excitation energy of the resulting compound nucleus in the hot fusion reaction ^{48}Ca+^{248}Cm.

tions considered. The contribution to the variance of TKE due to the nucleon exchange is more important in the decay of more asymmetric DNS. With increasing excitation energy, the variance of the TKE of quasifission products with A_P

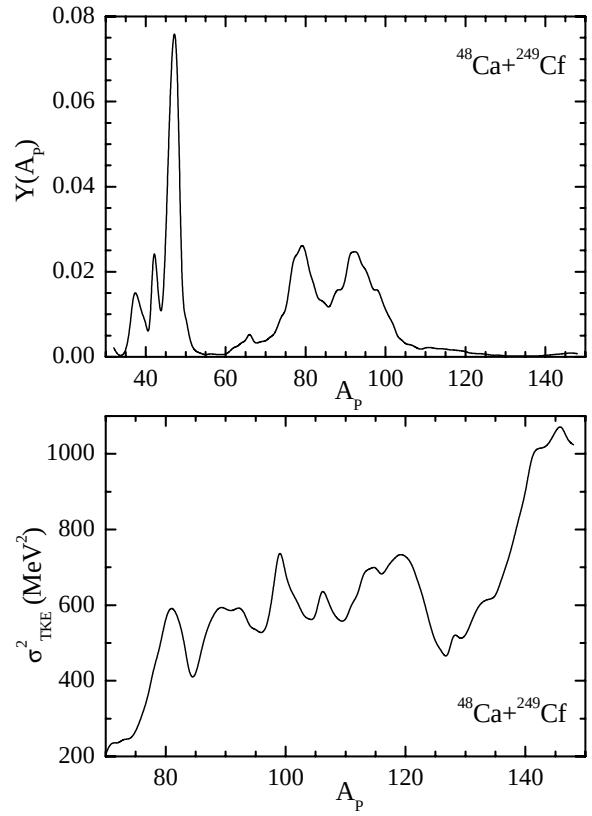

FIG. 7. The same as in Fig. 2, but for the hot fusion reaction ^{48}Ca+^{249}Cf$\rightarrow^{297}$118 at the bombarding energy corresponding to an excitation energy of the compound nucleus of 30.6 MeV.

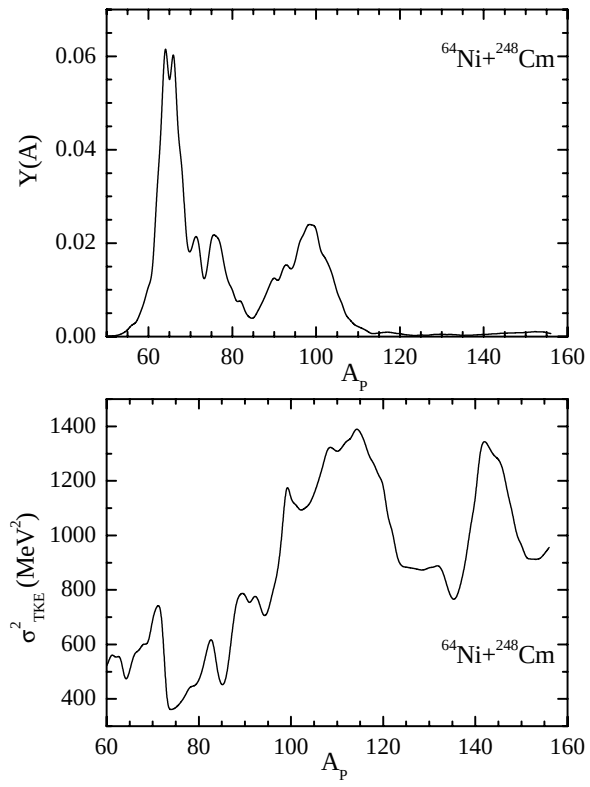

FIG. 8. The same as in Fig. 2, but for the hot fusion reaction ^{64}Ni+^{248}Cm$\rightarrow{}^{312}$124 at the bombarding energy corresponding to an excitation energy of the compound nucleus of 50 MeV.

$=A_{tot}/2\pm 20$ smoothly increases (Fig. 6), mainly due to the increase of $\sigma^2_{\beta_i}$ with Θ in Eq. (27).

Besides the maximum in $Y(A_P)$ corresponding to Pb as a heavy fragment, the maximum corresponding to the neutron number $N=50$ in the light fragment is also pronounced in the calculations for the reactions ^{48}Ca+^{248}Cm (Fig. 4) and ^{48}Ca+^{249}Cf (Fig. 7).

In Fig. 8, we show $Y(A_P)$ and $\sigma^2_{TKE}(A_P)$ for the ^{64}Ni +^{248}Cm reaction. Here, the yield of symmetric fragments is smaller than in Fig. 4, because the probability of the decay of asymmetric DNS configurations is larger due to a larger Coulomb repulsion and smaller values of quasifission barriers. In Fig. 8, the value of σ^2_{TKE} for symmetric products is smaller than in Fig. 4, because of the smaller excitation energies of the DNS at symmetric splitting.

2. Reactions with ^{58}Fe beam

Figures 9–13 show the calculated results for the reactions ^{58}Fe+^{232}Th, ^{244}Pu, ^{248}Cm, and ^{249}Cf which agree quite well with the available experimental data [1]. As in the reactions with ^{48}Ca, the calculated curves have more pronounced structures than the experimental data. In Fig. 11, one can see that the decay of the DNS consisting of stiff nuclei such as Ni, Sn, and Pb lead to minimal variances of the TKE. The average values of the variances of the TKE of quasifission products with $A_{tot}/2-20\leqslant A_P\leqslant A_{tot}/2$ are listed in Table I for various reactions. The relative yield of the quasifission products with $A_P>80$ decreases with increasing charge number of the target. The symmetric quasifission in the ^{58}Fe +^{249}Cf reaction is minimal among all considered reactions with ^{58}Fe.

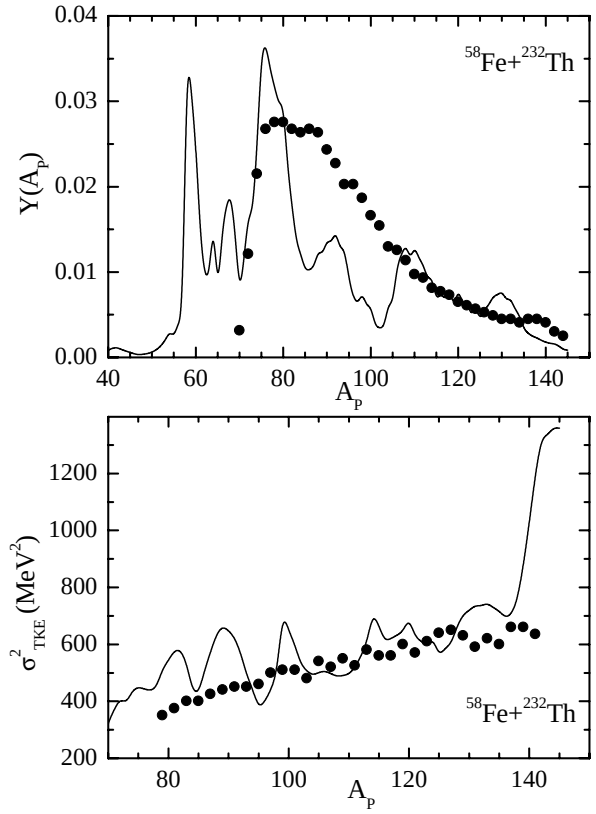

FIG. 9. The same as in Fig. 2, but for the hot fusion reaction ^{58}Fe+^{232}Th$\rightarrow{}^{290}$116 at the bombarding energy corresponding to an excitation energy of the compound nucleus of 53 MeV.

B. Cold fusion reactions

The calculations of quasifission products for the cold fusion reactions are important for the planned quasifission experiments in many laboratories. Figures 14–17 show the quasifission distributions of mass and the variance of the TKE for the cold fusion reactions ^{58}Fe, ^{64,70}Ni, and ^{86}Kr +^{208}Pb [20]. The dependences $Y(A_P)$ and $\sigma^2_{TKE}(A_P)$ are in quite good agreement with available experimental data [1]. The maxima of $Y(A_P)$ at $A_P=118-130$ are related to Sn isotopes in the DNS and correspond to the minima of the potential energy as a function of A_P.

Since the quasifission barrier $B_{qf}(Z,N)$ increases with decreasing Z and increasing number of neutrons in the system, the difference between the quasifission distributions in cold and hot fusion reactions is related to different choices of the colliding nuclei. We found for the reaction ^{86}Kr+^{208}Pb $\rightarrow{}^{294}$118 that the quasifission products are practically associated with fragmentations near the initial DNS due to small values of the quasifission barriers B_{qf}. In the Pb-based reactions, the relative yield of nearly symmetric quasifission fragments decreases with increasing atomic number of the projectile and is, in general, smaller than in the actinide-based reactions with ^{48}Ca.

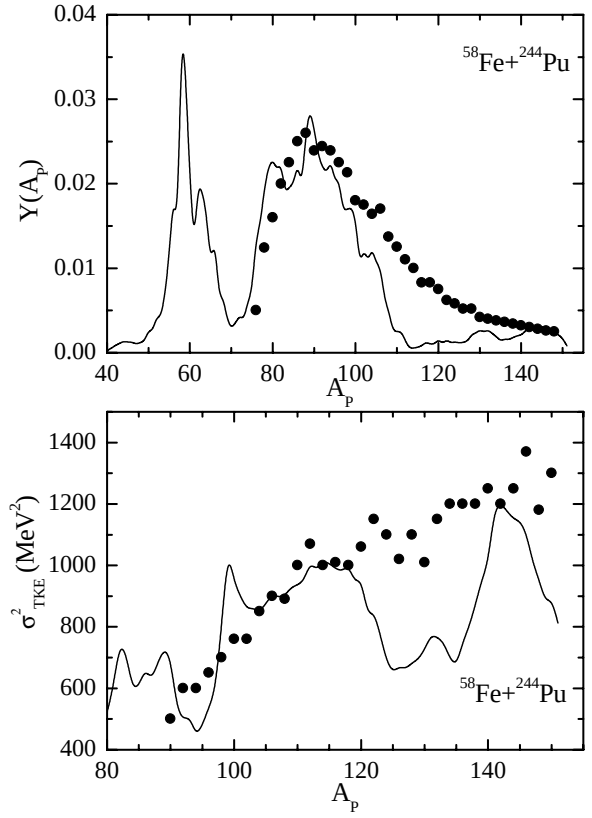

FIG. 10. The same as in Fig. 2, but for the hot fusion reaction ^{58}Fe+^{244}Pu→^{302}120 at the bombarding energy corresponding to an excitation energy of the compound nucleus of 44 MeV.

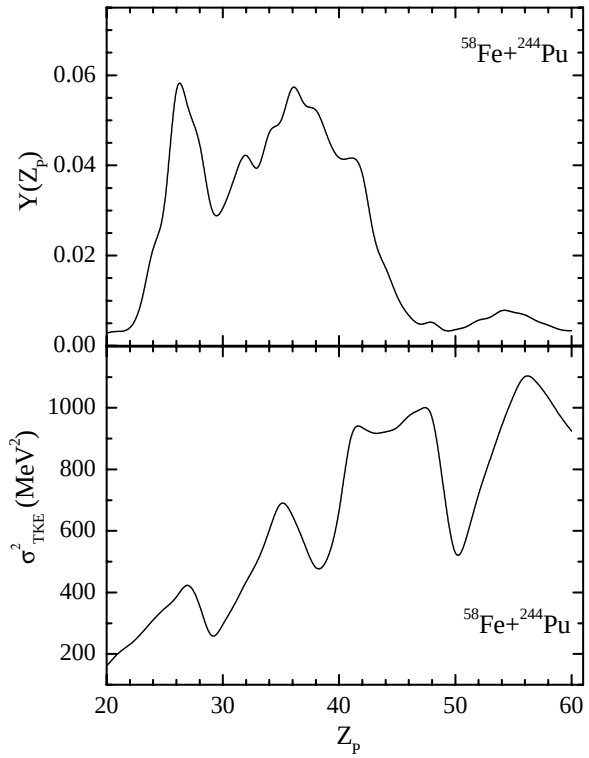

FIG. 11. Calculated charge yield (upper part) and variance of the TKE (lower part) of the quasifission products as a function of the atomic number of the light fragment for the hot fusion reaction ^{58}Fe+^{244}Pu→^{302}120 at the bombarding energy corresponding to an excitation energy of the compound nucleus of 44 MeV.

The yield of symmetric products of quasifission increases with increasing number of neutrons in the system due to larger values of B_{qf}. The dependence of $\sigma^2_{TKE}(A_P)$ on the neutron number of the projectile is, in general, rather weak (see Figs. 15 and 16). With increasing number of neutrons, the variance of TKE can be changed due to the change in stiffness of the nuclei in the DNS and due to the dependence of DNS excitation energy on A_P. In the ^{64}Ni+^{208}Pb reaction, the value of $\sigma^2_{TKE}(A_P \approx A_{tot}/2)$ is smaller than in the ^{70}Ni+^{208}Pb reaction, which is explained by a larger fraction of the DNS with the stiff nucleus ^{136}Xe. Indeed, the nucleus ^{136}Xe is two times stiffer than ^{138}Xe appearing the reaction with ^{70}Ni.

For the ^{86}Kr+^{198}Pt reaction, we demonstrate in Fig. 18 that the calculated mass distribution of quasifission products with maxima at $A_P=70-90$ and 100–110 well correspond to the minima or flat regions of the driving potential. The barrier of 22 MeV prohibits the motion of the initial DNS in mass asymmetry towards the compound nucleus. Due to this barrier, the probability to find the DNS with $A_P<60$ is very small and quasifission mainly results with products of $60<A_P<130$.

C. Quasifission in lighter systems

For $E_{\text{c.m.}}=225$ MeV in the ^{132}Xe+^{56}Fe reaction, one can take $J_{cap}=110$ and estimate σ_{cap} as 900 mb. The calculated quasifission cross sections σ_{qf} as a function of Z (Fig. 19) is in good agreement with the experimental data presented in Ref. [2], especially near $Z=40$. For example, the calculated $\sigma_{qf}(Z=38-40)\approx 82$ mb and the experiment gives about 90 mb. The cross section of fusion fission is estimated as $\sigma=\sigma_{cap}P_{CN}=40$ mb that contributes $\sigma_{ff}(A_P\approx A_{tot}/2)=\sigma/\sqrt{2\pi\sigma_A^2}=1.3$ mb to the symmetric splitting at the variance $\sigma_A^2=150$ of mass distribution. Thus, in this reaction the quasifission mainly leads to products with $Z=36-40$. We should note that experimental data were not shown in Fig. 19 for $Z<36$, because it was difficult to discriminate the quasifission events from the deep-inelastic events near the initial masses in the entrance channel.

In the ^{40}Ar+^{165}Ho reaction at $E_{\text{c.m.}}=155$ MeV, we found good agreement between the calculated and experimental values of the full width half maximum of the symmetric mass distribution, namely, 30 and experimental 38 ± 4 [3], respectively.

D. Competition between fusion-fission and quasifission processes in the yield of symmetric fragments

The relative contributions of the fusion fission with respect to the quasifission to the yield of symmetric products are listed in Table I for various reactions. The contribution of fusion fission is mainly determined by the fusion probability P_{CN}, since the survival probability of excited compound nucleus is much less than unity. Although this contribution increases with bombarding energy, it remains quite small in

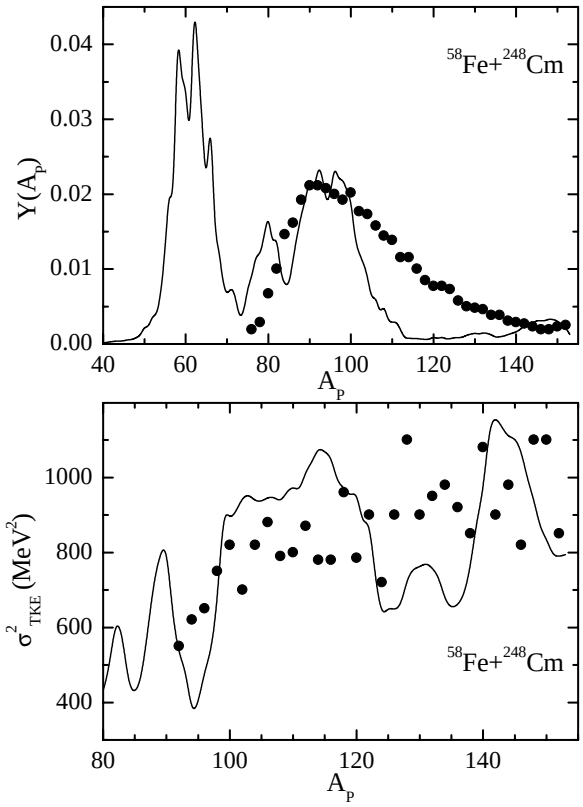

FIG. 12. The same as in Fig. 2, but for the hot fusion reaction ^{58}Fe+ ^{248}Cm$\rightarrow$ ^{306}122 at the bombarding energy corresponding to an excitation energy of the compound nucleus of 33 MeV.

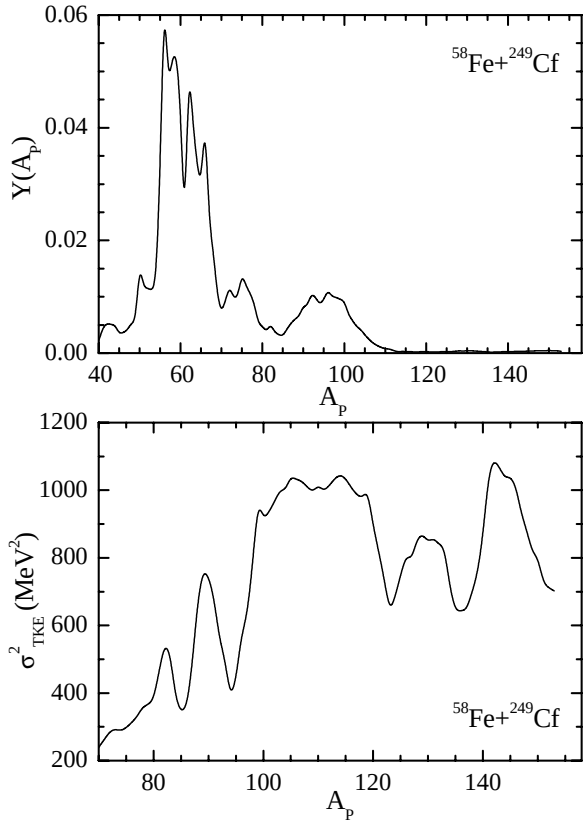

FIG. 13. The same as in Fig. 2, but for the hot fusion reaction ^{58}Fe+ ^{249}Cf$\rightarrow$ ^{307}124 at the bombarding energy corresponding to an excitation energy of the compound nucleus of 33 MeV.

the reactions considered. Therefore, in these reactions the quasifission mainly gives the yield of nearly symmetric products. The small contribution of fusion fission to nearly symmetric products was also obtained in Ref. [45] for few reactions without the description of the observable characteristics of quasifission. The ratio between the motions of the DNS to more asymmetric and more symmetric configurations depends on the initial mass asymmetry in the entrance channel and decreases exponentially with increasing charge number of the superheavy compound nucleus.

For example, for the reaction ^{48}Ca($E_{\rm c.m.}=193$ MeV) $+^{238}$U (Fig. 2), the calculated cross section of the yield of quasifission fragments with mass numbers $A_{tot}/2\pm 20$ is about 4.5 mb at $J_{cap}=25$, in good agreement with the measured value of about 5 mb [5]. For larger energy $E_{\rm c.m.}=216$ MeV, at $J_{cap}=80$ we have $\sigma_{qf}(A_P\approx A_{tot}/2)=2.9$ mb. At this energy we find $P_{CN}=1.35\times 10^{-2}$ and, therefore, the contribution of the fusion-fission mechanism to the fusion-fission cross section of symmetric fragments is $\sigma_{ff}(A_P\approx A_{tot}/2)=\sigma_{cap}P_{CN}/\sqrt{2\pi\sigma_A^2}\approx 0.1$ mb at the mass variance $\sigma_A^2=1000$.

E. Fission of the heavy nucleus in the DNS in hot fusion reactions

In actinide-based hot fusion reactions, there is the possibility of fission of heavy nucleus in the DNS. Since the fissility increases with the charge number of the nucleus, the fission of the heavy nucleus in the DNS can effect the quasifission and fusion when the DNS moves towards larger mass asymmetry (smaller A_P). We estimate the probability $Y_{fis}(A_P)$ of the fission of the heavier nucleus of the DNS as follows:

$$Y_{fis}(A_P)=\sum_Z \int_0^{t_0} P_{Z,A_P-Z}(t)\Lambda^{fis}_{Z_{tot}-Z,N_{tot}-A_P+Z}(t)dt. \tag{28}$$

Assuming the transient time to be small, the fission rate is changed by its quasistationary value estimated with the Kramers formula

$$\Lambda^{fis}_{Z,N}(\Theta)=\frac{1}{2\pi}\frac{\omega_{gs}}{\omega_f}\left(\sqrt{\left(\frac{\Gamma_0}{2\hbar}\right)^2+\omega_f^2}-\frac{\Gamma_0}{2\hbar}\right)\times\exp[-B_f(Z,N)/\Theta(Z,N)], \tag{29}$$

where ω_{gs} and ω_f are the frequencies of the oscillators approximating the fission-path potential at the ground state and on top of the fission barrier, respectively, in a nucleus with Z and N. For our estimates, we take $\hbar\omega_{gs}=\hbar\omega_f=0.5$ MeV, $\Gamma_0=2$ MeV, and the fission barrier $B_f(Z,N)$ is calculated as a sum of a liquid drop part [46] and shell corrections used in Ref. [47].

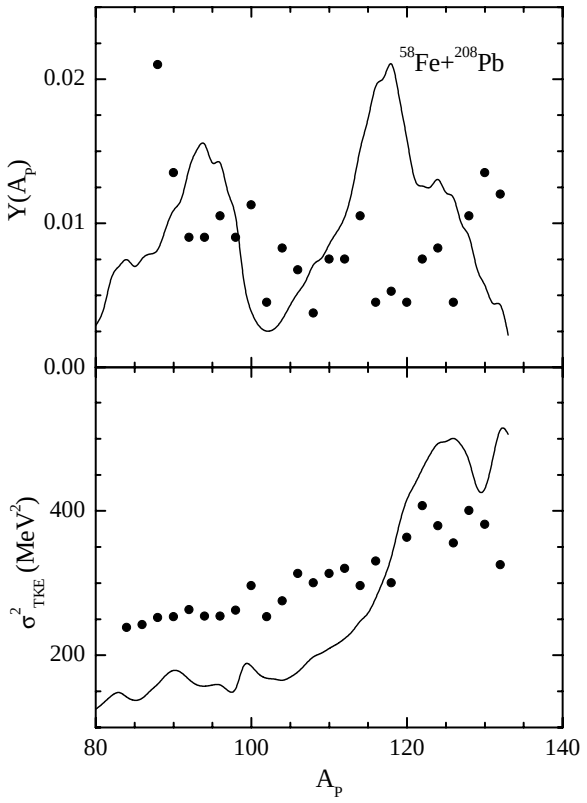

FIG. 14. The same as in Fig. 2, but for the cold fusion reaction ^{58}Fe+^{208}Pb$\rightarrow^{266}$108 at the bombarding energy corresponding to an excitation energy of the compound nucleus of 14.5 MeV.

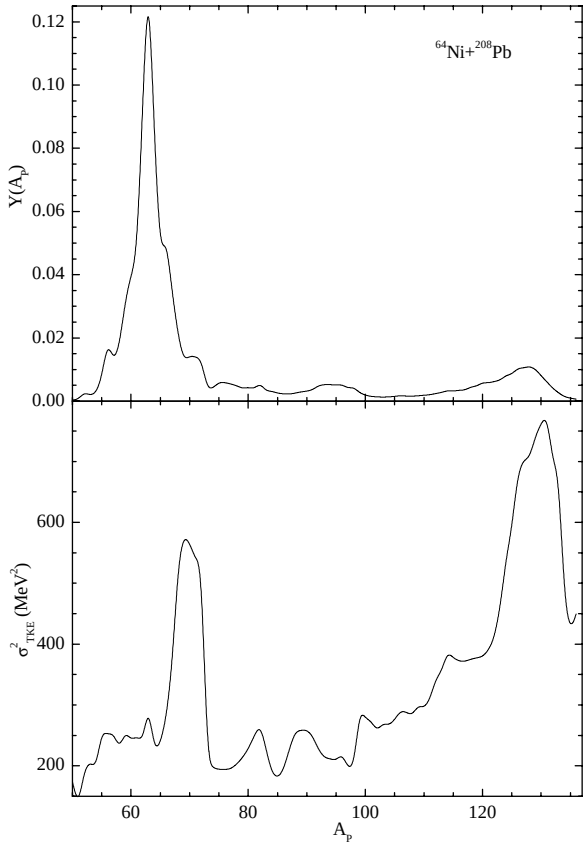

FIG. 15. The same as in Fig. 2, but for the cold fusion reaction ^{64}Ni+^{208}Pb$\rightarrow^{272}$110 at the bombarding energy corresponding to an excitation energy of the compound nucleus of 20 MeV.

The probability of fission of a heavy nucleus increases with its charge number and excitation energy. Since in all the considered reactions the DNS excitation energy and $P_{Z,N}$ decrease with increasing mass asymmetry with respect to the initial DNS, the fission in the DNS is mainly visible near the initial configuration. More symmetric DNS configurations consist of nuclei with quite large fission barriers, which prohibits the fission at the excitation energies considered.

While in the ^{48}Ca+^{248}Cm reaction $\Sigma_{A_P} Y_{fis}(A_P) \approx 0.012$ at the bombarding energy corresponding to $E^*_{CN}=50$ MeV, $\Sigma_{A_P} Y_{fis}(A_P) \approx 0.035$ in the ^{48}Ca+^{249}Cf reaction at the same excitation energy E^*_{CN} (Fig. 20). Therefore, the fission in the DNS is perceptible in the reactions where one of the partners has $Z>96$ and $E^*_{CN}>30$ MeV. For $E_{\text{c.m.}}$ corresponding to $E^*_{CN}=33$ MeV, $\Sigma_{A_P} Y_{fis}(A_P) \approx 0.007$ and 0.03 in the reactions ^{48}Ca+^{248}Cm and ^{48}Ca+^{249}Cf, respectively. In these reactions we have $\Sigma_{A_P=A_{tot}/2\pm 20} Y(A_P)=0.08$ and 0.02, respectively. Therefore, in the reactions with targets with $Z>96$, the fission of the heavy nucleus in the DNS with a consequent fusion of one of the fission fragments with the projectilelike DNS nucleus can sufficiently contribute to the yield of symmetric products, resulting from two-body processes of complete momentum transfer. For example, if ^{248}Cm is split up into ^{108}Mo and ^{140}Xe, ^{108}Mo+^{48}Ca forms ^{156}Sm, which we observe together with ^{140}Xe. The TKE of one of the fission fragments and the other nucleus (="other fission fragment"+"projectile-like nucleus") is about 25 MeV smaller than the average TKE of quasifission products.

F. Preneutron and postneutron emission

Assuming a small number of neutrons emitted from the DNS before it decays, we estimate this number as follows:

$$\langle M_n^{pre}\rangle(A_P)=\sum_Z \int_0^{t_0} P_{Z,A_P-Z}(t)[\lambda^n_{Z,A_P-Z}(t) + \lambda^n_{Z_{tot}-Z,N_{tot}-A_P+Z}(t)]dt, \quad (30)$$

where we use the quasistationary rate of neutron emission from the two DNS nuclei:

$$\lambda^n_{Z,N}=\frac{[\Theta(Z,N)]^2(Z+N)^{2/3}}{20\pi}\exp[-B_n(Z,N)/\Theta(Z,N)]. \quad (31)$$

Here, $B_n(Z,N)$ is the binding energy of a neutron in the DNS nucleus with mass number $A_P=Z+N$ and we assume that the excitation energy of the DNS is distributed between nuclei proportionally to their masses $[\Theta(Z,N)=\Theta(Z_{tot}-Z,N_{tot}-N)]$.

After the decay of the DNS, the number of neutrons emitted from the nuclei is calculated as

$$\langle M_n^{post}\rangle(A_P)=\frac{A_P}{A_{tot}}\sum_Z\frac{Y_{Z,A_P-Z}(t_0)E^*(Z,N)}{\langle B_n(Z,A_P-Z)+2\Theta(Z,A_P-Z)\rangle}+\frac{A_{tot}-A_P}{A_{tot}}\sum_Z\frac{Y_{Z,A_P-Z}(t_0)E^*(Z,A_P-Z)}{\langle B_n(Z_{tot}-Z,N_{tot}-A_P+Z)+2\Theta(Z,A_P-Z)\rangle}, \quad (32)$$

where the DNS total excitation energy $E^*(Z,N)=E^*(Z_i,N_i)+[U(Z_i,N_i)-U(Z,N)]$ is obtained from the excitation energy $E^*(Z_i,N_i)$ of the initial DNS, and the difference of the potential energies of the initial DNS and of the DNS with A_P. Here, $\langle B_n(Z,N)+2\Theta(Z,N)\rangle$ is the average excitation energy carried by an emitted neutron from the light nucleus.

The calculated values of $\langle M_n^{pre}\rangle(A_P)$ and the total number of evaporated neutrons $\langle M_n^{tot}\rangle(A_P)=\langle M_n^{pre}\rangle(A_P)+\langle M_n^{post}\rangle(A_P)$ as functions of A_P are presented in Figs. 21 and 22 for the reactions ^{48}Ca, ^{58}Fe+^{244}Pu, and ^{248}Cm. Although the neutron emission from the DNS increases with the DNS excitation energy, it remains relatively small for all the reactions considered. The maxima of $\langle M_n^{pre}\rangle(A_P)$ correspond to the maxima of $Y(A_P)$, i.e., the DNS lives for a longer time. The calculated average total numbers of emitted neutrons for nearly symmetric quasifission splitting ($\langle M_n^{tot-sym}\rangle$) with $A_{tot}/2-20\leqslant A_P\leqslant A_{tot}/2$ and for the quasifission splitting ($\langle M_n^{tot-asym}\rangle$) with $A_P<A_{tot}/2-20$ are compared with the measured values in Fig. 23 for the reactions indicated.The theoretical data practically agree with the experimental data [1]. The calculated results on($\langle M_n^{tot-sym}\rangle$) and ($\langle M_n^{tot-asym}\rangle$) are summarized in Table I.

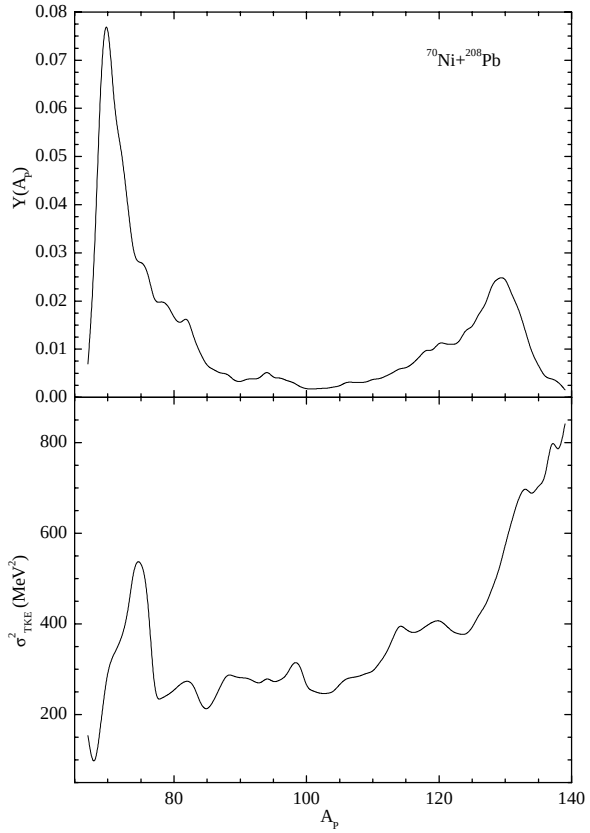

FIG. 16. The same as in Fig. 2, but for the cold fusion reaction ^{70}Ni+^{208}Pb→^{278}110 at the bombarding energy corresponding to an excitation energy of the compound nucleus of 20 MeV.

IV. SUMMARY

The main conclusions are the following:

(1) The diffusion in charge (mass) asymmetry and in relative distance (the DNS decay) coordinates contributes to the yields of quasifission products.

(2) The quasifission products of hot fusion actinide-based reactions with ^{48}Ca and ^{58}Fe projectiles are correctly described with the DNS model. The estimated variance of total kinetic energy of the quasifission products is in agreement with the experimental data. The calculations confirm the influence of shell effects on the DNS evolution. Indeed, the maxima of the quasifission yields correspond to the minima of the DNS potential energy as a function of mass asymmetry.

(3) For the cold fusion reactions leading to the superheavy elements, the quasifission products are practically associated with fragmentations near the initial (entrance) DNS. However, the increase of the neutron number in the DNS results in a larger fraction of nearly symmetric splitting.

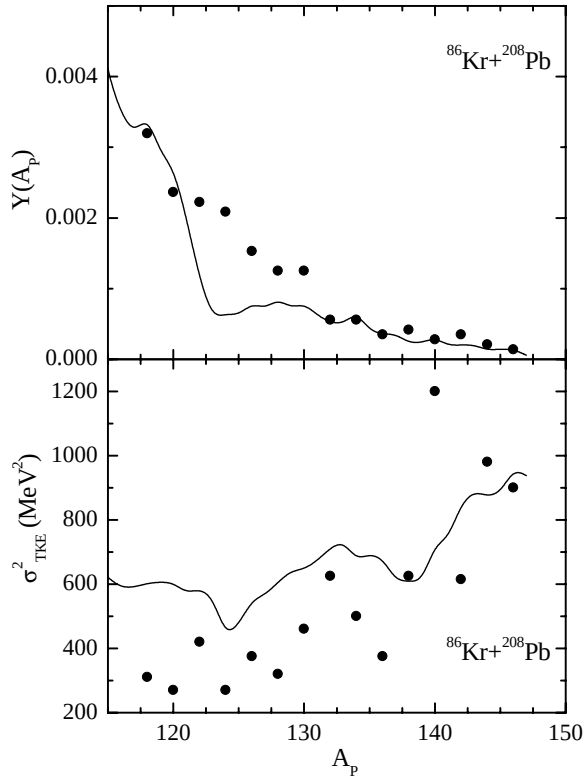

FIG. 17. The same as in Fig. 2, but for the cold fusion reaction ^{86}Kr+^{208}Pb→^{294}118 at the bombarding energy corresponding to an excitation energy of the compound nucleus of 17 MeV.

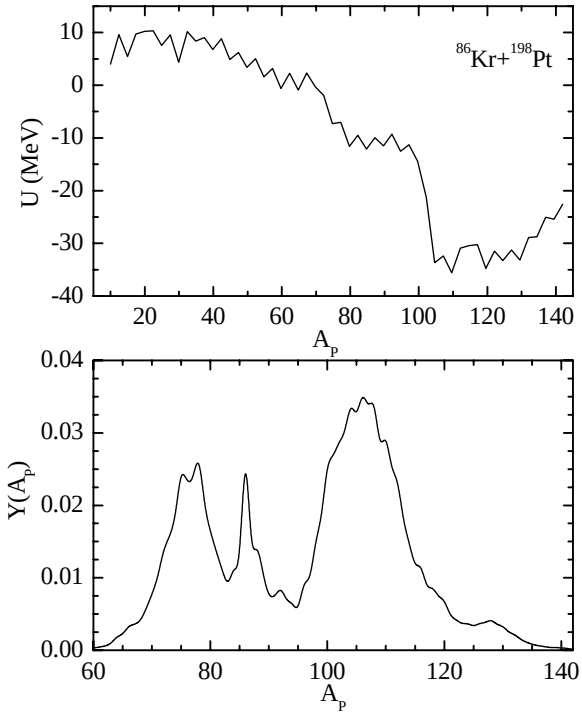

FIG. 18. Upper part: Calculated potential energy of the DNS as a function of the mass number of the light fragment for the ^{86}Kr $+^{198}$Pt reaction at $J=0$. The deformation parameters are taken from Ref. [40] for the nuclei of the DNS. The potential energy is minimized with respect to the N/Z ratio, $A_P=Z+N$. Lower part: Mass yield of the quasifission products as a function of A_P for the cold fusion reaction ^{86}Kr$+^{198}$Pt$\rightarrow^{284}$114 at a bombarding energy corresponding to an excitation energy of the compound nucleus of 25 MeV.

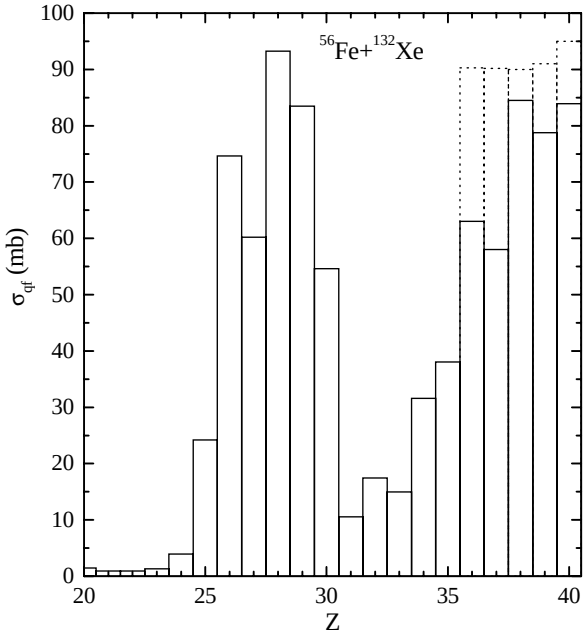

FIG. 19. Calculated (solid lines) cross sections for the quasifission products as a function of the atomic number of the light fragment for the reaction ^{132}Xe$+^{56}$Fe at $E_{\mathrm{c.m.}}=225$ MeV. The experimental data [2] are shown by dashed lines.

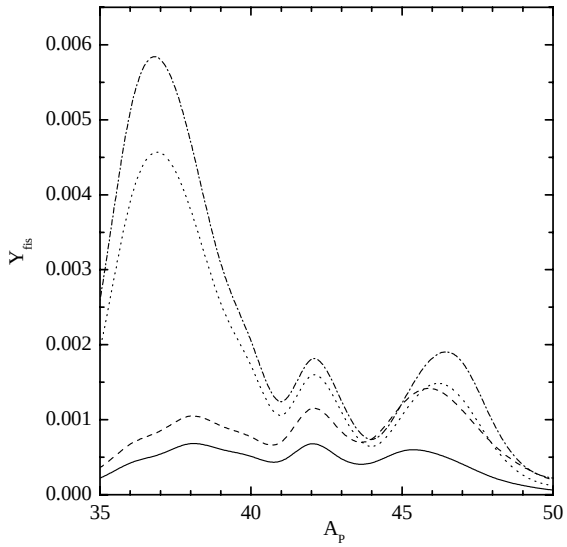

FIG. 20. Calculated probabilities of fission of the heavy nucleus in the DNS as a function of the mass number of the light DNS nucleus. The results for the ^{48}Ca$+^{248}$Cm reaction at $E^*_{CN}=37$ and 50 MeV are presented by solid and dashed curves, respectively. The results for the ^{48}Ca$+^{249}$Cf reaction at $E^*_{CN}=30.6$ and 50 MeV are presented by dotted and dash-dotted curves, respectively.

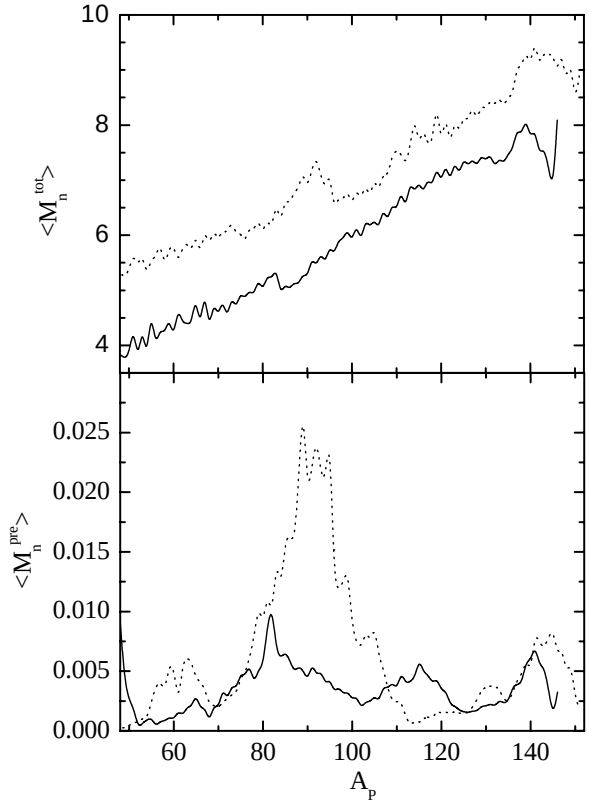

FIG. 21. Calculated total (upper part) and predecay (lower part) numbers of neutrons emitted in the reactions ^{48}Ca$+^{244}$Pu (solid lines) and ^{58}Fe$+^{244}$Pu (dashed lines) at the same energies as in Figs. 1 and 10.

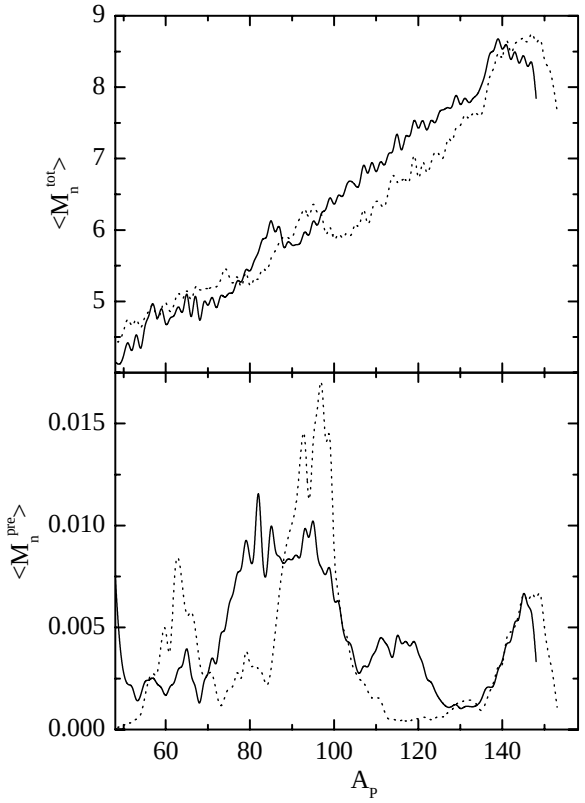

FIG. 22. The same as in Fig. 21, but for the reactions ^{48}Ca $+^{248}$Cm (solid lines) and ^{58}Fe$+^{248}$Cm (dashed lines) at the same energies as in Figs. 4 and 12.

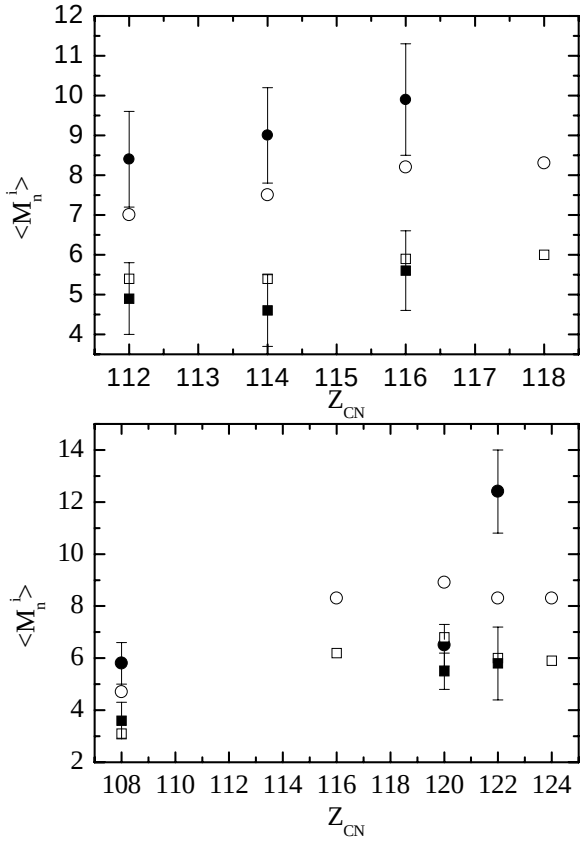

FIG. 23. Calculated average total numbers of neutrons emitted from the quasifission fragments with $A_{tot}/2-20 \leqslant A_P$ (open circles) and from the quasifission fragments with $A_P < A_{tot}/2-20$ (open squares) are compared with the experimental data presented by solid circles and squares, respectively. The results for the reactions ^{48}Ca$+^{238}$U, ^{244}Pu, ^{248}Cm, and ^{249}Cf are presented in the upper part. The results for the reactions ^{58}Fe$+^{208}$Pb, ^{232}Th, ^{244}Pu, ^{248}Cm, and ^{249}Cf are presented in the lower part. The bombarding energies are the same as the corresponding bombarding energies in Figs. 1, 2, 4, 7, 9, 10, 12, 13, 14.

(4) If the heavier reaction partner with $Z>96$ fissions, this fission with a following fusion of one fission fragment with the light nucleus of the DNS can be mixed with nearly symmetric quasifission.

(5) The number of neutrons emitted from the DNS (predecay neutrons) is very small in the reactions considered. The total number of neutrons from predecay and postdecay accompanying the quasifission is well described in our model.

(6) If the compound nucleus is quite stable to be detected, the quasifission process is the main factor suppressing the complete fusion of heavy nuclei. In fusion reactions, the fusion-fission events are much smaller than the events of the production of quasifission. The main contribution to symmetric and near symmetric fragmentations comes from quasifission.

(7) Since the quasifission dominates in the cold and hot fusion reactions, a comparison of theoretical and experimental data of the yields of asymmetric quasifission products constitutes a critical test for the dynamics of existing fusion models. The measurement of highly asymmetric quasifission products can prove the evolution of the DNS to the compound nucleus in the mass asymmetry coordinate.

ACKNOWLEDGMENTS

We thank Professor V. V. Volkov, Professor R. V. Jolos, Professor J. Peter, Dr. E. A. Cherepanov, Dr. A. K. Nasirov, and A. V. Andreev for fruitful discussions and suggestions. G.G.A. and N.V.A. are grateful for the support of the Alexander von Humboldt-Stiftung. This work was supported in part by Volkswagen-Stiftung, DFG and RFBR, and STCU (Grant No. Uzb-45). The Polish-JINR (Dubna) and IN2P3 (France)–JINR (Dubna) Cooperation Program are gratefully acknowledged.

[1] M. G. Itkis *et al.*, *JINR*, Report No. E15-99-248 1999; *Proceedings of the Seventh International Conference on Clustering Aspects of Nuclear Structure and Dynamics*, edited by M. Korolija, Z. Basrak, and R. Caplar (World Scientific, Singapore, 2000), p. 386; in *Proceedings of the International Symposium on Exotic Nuclei*, edited by Yu. E. Penionzhkevich and E. A. Cherepanov (World Scientific, Singapore, 2001), p. 143; in *Proceedings of the International Conference on*

Nuclear Physics at Border Lines, edited by G. Fazio *et al.*, (World Scientific, Singapore, 2002), p. 146; I. M. Itkis *et al.*, *Proceedings of the International Conference on Nuclear Physics at Border Lines*, edited by G. Fazio *et al.* (World Scientific, Singapore, 2002), p. 142; E. M. Kozulin *et al.*, *ibid.*, p. 157.
[2] B. Heusch *et al.*, Z. Phys. A **288**, 391 (1978).
[3] C. Lebrun *et al.*, Nucl. Phys. **A321**, 207 (1979); B. Borderie *et al.*, Z. Phys. A **299**, 263 (1981).
[4] B.B. Back *et al.*, Phys. Rev. Lett. **46**, 1068 (1981); **50**, 818 (1983); R. Bock *et al.*, Nucl. Phys. **A388**, 334 (1982); M.B. Tsang *et al.*, Phys. Lett. **129B**, 18 (1983); Z. Zheng *et al.*, Nucl. Phys. **A422**, 447 (1984); G. Guarino *et al.*, **A424**, 157 (1984); P. Gippner *et al.*, Phys. Lett. B **252**, 198 (1990).
[5] J. Toke *et al.*, Nucl. Phys. **A440**, 327 (1985).
[6] W.Q. Shen *et al.*, Phys. Rev. C **36**, 115 (1987).
[7] Ch. Ngo, Prog. Part. Nucl. Phys. **16**, 139 (1986).
[8] V.V. Volkov, Phys. Rep. **44**, 93 (1978); *Nuclear Reactions of Deep Inelastic Transfers* (Energoizdat, Moscow, 1982).
[9] W. U. Schröder and J. R. Huizenga, in *Treatise on Heavy-Ion Science*, edited by D. A. Bromley (Plenum Press, New York, 1984), Vol. 2, p. 115.
[10] J. Randrup, Nucl. Phys. **A307**, 319 (1978); **A327**, 490 (1979).
[11] G.G. Adamian, A.K. Nasirov, N.V. Antonenko, and R.V. Jolos, Phys. Part. Nucl. **25**, 583 (1994).
[12] V.V. Volkov, Izv. Akad. Nauk SSSR, Ser. Fiz. **50**, 1879 (1986).
[13] G.G. Adamian, N.V. Antonenko, and W. Scheid, Nucl. Phys. **A618**, 176 (1997); G.G. Adamian, N.V. Antonenko, W. Scheid, and V.V. Volkov, *ibid.* **A627**, 361 (1997); **A633**, 409 (1998); E. A. Cherepanov, JINR, Report No. E7-99-27 1999; R.V. Jolos, A.K. Nasirov, and A.I. Muminov, Eur. Phys. J. A **4**, 245 (1999).
[14] G.G. Adamian, N.V. Antonenko, and W. Scheid, Nucl. Phys. **A678**, 24 (2000).
[15] A. K. Nasirov *et al.*, in *Proceedings of the XIV International Workshop on Nuclear Fission Physics, Obninsk*, (GNTs RFFEhI, Obninski, 2000), p. 106.
[16] A. Diaz-Torres, G.G. Adamian, N.V. Antonenko, and W. Scheid, Phys. Rev. C **64**, 024604 (2001).
[17] A. Diaz-Torres, G.G. Adamian, N.V. Antonenko, and W. Scheid, Nucl. Phys. **A679**, 410 (2001).
[18] W. von Oertzen, Z. Phys. A **342**, 177 (1992).
[19] G.G. Adamian, N.V. Antonenko, and Yu.M. Tchulvil'sky, Phys. Lett. B **451**, 289 (1999); G.G. Adamian, N.V. Antonenko, S.P. Ivanova, and W. Scheid, Nucl. Phys. **A646**, 29 (1999); A. Diaz-Torres, N.V. Antonenko, and W. Scheid, *ibid.* **A652**, 61 (1999); A. Diaz-Torres, G.G. Adamian, N.V. Antonenko, and W. Scheid, Phys. Lett. B **481**, 228 (2000); G.G. Adamian, N.V. Antonenko, A. Diaz-Torres, and W. Scheid, Nucl. Phys. **A671**, 233 (2000).
[20] S. Hofmann and G. Münzenberg, Rev. Mod. Phys. **72**, 733 (2000).
[21] Yu.Ts. Oganessian *et al.*, Eur. Phys. J. A **5**, 63 (1999); Phys. Rev. Lett. **83**, 3154 (1999); A.V. Yeremin, V.K. Utyonkov, and Yu.Ts. Oganessian, in *Tours Symposium on Nuclear Physics III*, edited by M. Arnould, M. Lewitowicz, Yu. Ts. Oganessian, M. Ohta, H. Utsunomiya, and T. Wada, AIP Conf. Proc. No. 425 (AIP, Woodbury, NY, 1998), p. 16.
[22] Yu.Ts. Oganessian *et al.*, Phys. Rev. C **62**, 041604(R) (2000).
[23] N.V. Antonenko and R.V. Jolos, Yad. Fiz. **50**, 98 (1989) [Sov. J. Nucl. Phys. **50**, 62 (1989)]; Z. Phys. A **338**, 423 (1991).
[24] G.G. Adamian, N.V. Antonenko, R.V. Jolos, and A.K. Nasirov, Nucl. Phys. **A551**, 321 (1993).
[25] V. G. Solovev, *Theory of Complex Nuclei* (Nauka, Moscow, 1971); V.A. Chepurnov, Yad. Fiz. **6**, 955 (1967).
[26] G.G. Adamian, R.V. Jolos, and A.K. Nasirov, Yad. Fiz. **55**, 651 (1992) [Sov. J. Nucl. Phys. **55**, 366 (1992)].
[27] A.M. Wapstra and G. Audi, Nucl. Phys. **A432**, 1 (1985).
[28] P. Möller and R. Nix, At. Data Nucl. Data Tables **39**, 213 (1988).
[29] A. Krasznahorkay *et al.*, Phys. Rev. Lett. **80**, 2073 (1998); P.G. Thirolf and D. Habs, Prog. Part. Nucl. Phys. **49**, 325 (2002).
[30] J.F. Berger, M. Girod, and D. Gogny, Nucl. Phys. **A502**, 85c (1989); M.K. Pal, *ibid.* **A556**, 201 (1993); K. Rutz *et al.*, *ibid.* **A590**, 680 (1994); A. Sobiczewski *et al.*, *ibid.* **A473**, 77 (1987); V.V. Pashkevich, *ibid.* **A169**, 275 (1971); P. Möller, S.G. Nilsson, and R.K. Sheline, Phys. Lett. **40B**, 329 (1972).
[31] V. M. Strutinsky, in *Proceedings of the Second International Symposium on Physics and Chemistry of Fission* (IAEA, Vienna, 1969), p. 155.
[32] H.A. Kramers, Physica **7**, 284 (1940); V.M. Strutinsky, Phys. Lett. **47B**, 121 (1973).
[33] P. Grangé *et al.*, Phys. Rev. C **27**, 2063 (1983); P. Grangé, Nucl. Phys. **A428**, 37c (1984).
[34] P. Fröbrich and G.R. Tillack, Nucl. Phys. **A540**, 353 (1992).
[35] G.G. Adamian, N.V. Antonenko, and R.V. Jolos, Nucl. Phys. **A584**, 205 (1995).
[36] I.I. Gonchar and G.I. Kosenko, Sov. J. Nucl. Phys. **53**, 133 (1991).
[37] A. V. Andreev *et al.* (unpublished).
[38] P.D. Wilkins, E.P. Steinberg, and R.R. Chasman, Phys. Rev. C **14**, 1832 (1976).
[39] A. Bohr and B. Mottelson, *Nuclear Structure* (W. A. Benjamin, New York, 1974), Vol. 2.
[40] S. Raman, C.W. Nester, and P. Tikkanen, At. Data Nucl. Data Tables **78**, 1 (2001).
[41] D.J. Hinde, D. Hilscher, and H. Rossner, Nucl. Phys. **A502**, 497c (1989).
[42] V.E. Viola, Nucl. Data A **1**, 391 (1966); V.E. Viola, K. Kwiatkowski, and M. Wolker, Phys. Rev. C **31**, 1550 (1985).
[43] J. P. Unik *et al.*, in *Proceedings of the International Conference on Physics and Chemistry of Fission* (IAEA, Vienna, 1974), p. 19.
[44] R.T. Souza *et al.*, Phys. Rev. C **37**, 1901 (1988); **39**, 114 (1989).
[45] Y. Aritomo and M. Ohta, in *Proceedings of the Symposium on Nuclear Clusters*, edited by R. Jolos and W. Scheid (EP Systema, Debrecen, 2003), p. 391.
[46] V.S. Barashenkov *et al.*, Nucl. Phys. **A206**, 131 (1973).
[47] G.G. Adamian *et al.*, Phys. Rev. C **62**, 064303 (2000); A.S. Zubov *et al.*, *ibid.* **65**, 024308 (2002).